Master Thesis

The role of isopycnal mixing for tracer uptake in the global ocean

Ashwita Chouksey

Matriculation number: 6933339

Jabalpur, India

Fakultät für Mathematik, Informatik und Naturwissenschaften

Institut für Meereskunde

Universität Hamburg

Hamburg, 20 May 2019

Supervisors
Dr. Alexa Griesel
Prof. Dr. Carsten Eden

Abstract

This thesis addresses the role of isopycnal mixing in the tracer uptake and overturning circulation. To achieve this a global non-eddy- resolving model configuration of the Python Ocean Model 2.1 is implemented with a horizontal resolution of $\sim 2^\circ \times 2^\circ$. Four model setups are used, of which one setup uses a parameterized isopycnal diffusivity based on Eden-Greatbatch mesoscale eddy closure, and the other three setups use constant isopycnal diffusivities of 1000 m^2/s, 2000 m^2/s , and 5000 m^2/s.

The results show that an increasing isopycnal diffusivity makes the oceanic interior cooler and fresher, resulting in the weakening of the deep water formation. Consequently, the strength of the overturning circulation weakens, as seen in the volume transport associated with the North Atlantic Ocean, Southern Ocean as well as the Antarctic Circumpolar Current. In high latitudes, the isopycnal diffusion diffuses temperature and salinity upwards, and gradients of salinity on isopycnal surfaces are larger than those of temperature, so the isopycnal diffusive salinity flux is comparatively larger. This leads to cooling and freshening of the North Atlantic Deep Water and Antarctic Intermediate Water, and a decrease in the horizontal density gradient across the Antarctic Circumpolar Current. On the contrary, the parameterized isopycnal diffusivity makes the oceanic interior warmer and saltier, resulting in enhanced deep water formation shows and hence a stronger overturning circulation. Further, the impact of isopycnal diffusivity on the passive tracers is assessed with the age tracer, CFC-11, and CFC-12. In setups with a constant isopycnal diffusivity, with increasing diffusivity there is an increased uptake of CFC-11 and the ocean becomes more and more ventilated. On the other hand, the parameterized isopycnal diffusivity results in less CFC-11 uptake and the ocean is less ventilated. In all the setups, the tracer uptake is higher in the Southern Ocean. Therefore, the choice of isopycnal diffusivity in the model can significantly impact the deep water formation, overturning circulation, and the tracer uptake.

Contents

Chapter 1

Introduction

The tracer uptake by the ocean is an important oceanic process and has gained a lot of interest in the last decades. Several observational and model based studies have discussed and proposed the mechanisms of tracer uptake in the ocean. However, the parameters that control the uptake and distribution of the tracers still poses open questions. One such parameter is the isopycnal diffusivity, which results from the diffusive effect of the mesoscale eddies.

This thesis aims to address the sensitivity of tracer uptake by the ocean to the changes in isopycnal diffusivities. This provides further information on the changes in heat and salt transport and thus changes in the circulation, as well as on the changes in ventilation pathways. To address this question, a model of global resolution with non-eddy-resolving configuration is used to investigate the changes in tracer uptake and circulation using different values of isopycnal diffusivities. Four model setups are used in three of which the isopycnal diffusivity is kept constant and in the fourth the isopycnal diffusivity is parameterized using a mesoscale eddy closure. The results indicate significant changes in the transport and uptake of tracers as well as in the resulting overturning circulation.

1.1 Meridional Overturning Circulation (MOC)

The global ocean circulation is mainly driven by the Meridional Overturning Cicrculation (MOC) which essentially is the circulation of oceanic water masses in the meridional-vertical plane as shown in Fig. 1.1.

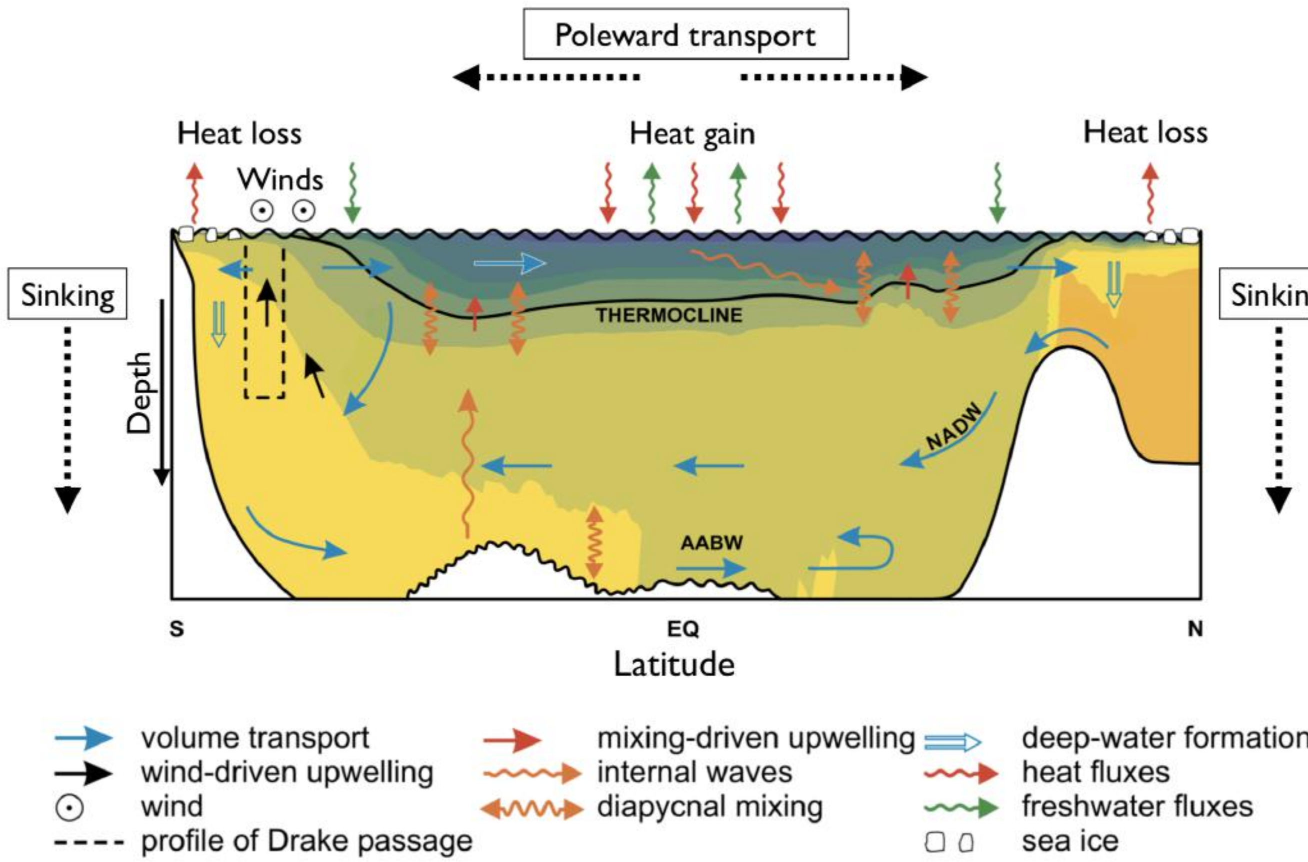

Figure 1.1: A schematic meridional section of the Atlantic Ocean representing a zonally averaged picture from Kuhlbrodt et al. (2007). The AMOC is denoted by straight blue arrows. Black arrows denote wind-driven upwelling due to the divergence of the surface winds in the Southern Ocean. The heat loss at high latitudes results in cooling and subsequent sinking, i.e. formation of the deep-water masses: North Atlantic Deep Water (NADW) and Antarctic Bottom Water (AABW).

The MOC is driven by two main mechanisms: wind and mixing. A simple view of the mixing-driven branch of the MOC is as follows: the warmer and lighter surface waters in the tropics are transported polewards by wind-driven surface currents, such as the Gulf Stream. At high latitudes, the waters become denser due to cooling and sink into the interior of the ocean. This results in the formation of deeper water masses, which are mixed upwards during their return in the MOC loop. This mixing lightens the deep water masses, which are cold and salty and hence dense, and causes them to eventually rise at low latitudes to complete the meridional loop.

1.2 Southern Ocean Circulation

The other major branch of the MOC is the wind-driven upwelling in the Southern Ocean (SO) (e.g. Toggweiler and Samuels (1998); Kuhlbrodt et al. (2007); Marshall and Speer (2012)). The properties of the abyssal ocean are mainly set by three sources, Antarctic Bottom Water (AABW), Circumpolar Deep Water (CDW), and Antarctic Intermediate Water (AAIW) (Gnanadesikan et al., 2007) which are formed in the SO, as shown in Fig. 1.2. The SO circulation is shaped by the Antarctic Circumpolar Current (ACC), mesoscale eddies, and the Ekman transport (Olbers et al., 2012). The ACC is controlled by local winds, buoyancy forcing and eddies (Rintoul et al., 2001). The ACC volume transport can also be increased by decreasing the rate of NADW formation (e.g. Fu**c**kar and Vallis (2007)) and decreased by increasing isopycnal mixing (Sévellec et al., 2010)
This cell ventilates the deep ocean and regulates the partitioning of CO_2 between the atmosphere and the ocean (Stewart et al., 2014). The upwelled water takes up a large amount of excess heat from the atmosphere because it is much colder. The upwelled water also takes up large amount of anthropogenic CO_2, because more CO_2 can be dissolved in the colder upwelled waters.

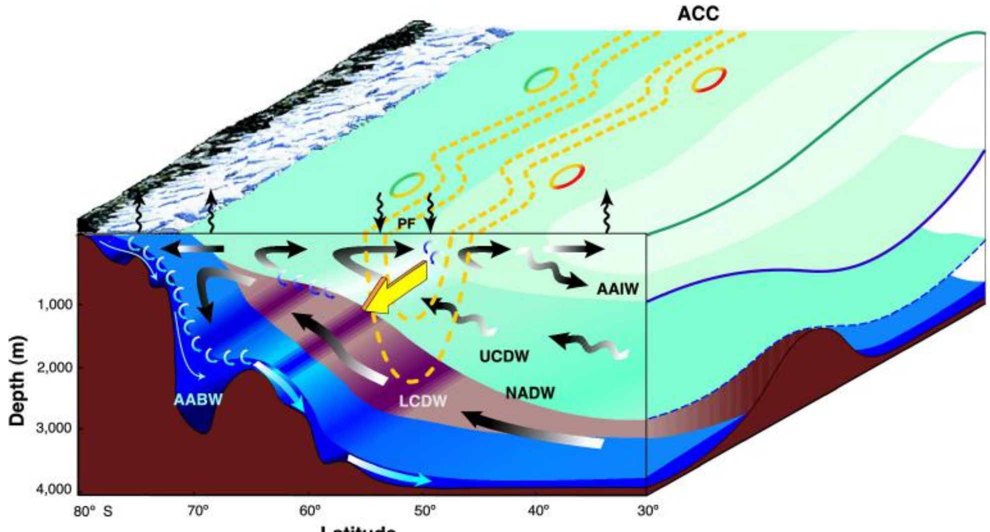

Figure 1.2: A sketch of the oceanic water masses. The figure is from Olbers and Visbeck (2005). The figure shows the zonal and meridional flow of the Antarctic Circumpolar Current (ACC). The slopes of isopycnals are shown with arrows attached, which representing turbulent mixing. The bouyancy flux is shown with curly arrows which are at the surface. The upper cell is primarily formed by Ekman and eddy transport in Upper Circumpolar Deep Water (UCDW) layer, and the lower cell is primarily driven by the dense Antarctic Bottom Water (AABW), and inflowing Lower Circumpolar Deep Water (LCDW) and North Atlantic Deep Water (NADW).

1.3 Tracer uptake in the ocean

The ocean takes up $\sim 40\%$ of the total anthropogenic Carbon (e.g. Sabine et al. (2004)). The Southern Ocean is a major region of uptake of anthropogenic carbon and heat. There are indications that SO ventilation has changed in the recent decades. The eddies have an important role to play in the CO_2 sink in the Southern Ocean (e.g. Sallée et al., 2012). Results from numerical modeling also show the prominent effect of eddies on the CO_2 storage and induced changes in the overturning circulation (e.g. Munday et al. (2014)). Numerical simulations of a passive ventilation tracer (CFCs or anthropogenic carbon-dioxide CO_2) demonstrate that the variations in tracer uptake across experiments are dominated by changes in isopycnal diffusivities (e.g. Dutay et al. (2002)). According to Dutay et al. (2002), the models with isopycnal diffusion and eddy-induced velocity parameterisation produce more realistic intermediate water ventilation, and an increased uptake of passive tracer. Using CFC data from observations, Waugh et al. (2013) demonstrated a decrease in the age of Subantarctic Mode Water (SAMW) and an increase in the age of Circumpolar Deep water (CDW), thus contributing to the understanding of the ventilation. A better understanding of the role isopycnal mixing would be more helpful in generating projections of carbon storage and feedbacks.

Isopycnal mixing has been discussed in past studies. Abernathey and Ferreira (2015) used a calculated isopycnal diffusivity with changing wind stress on tracer uptake, however the formulation of isopycnal diffusivity in their model is different from the formulation implemented in this thesis which is based on the mesoscale eddy closure by Eden and Greatbatch (2008). Their results show an increase in the the tracer uptake with increasing wind stress. Another study related to isopycnal diffusivity is by Sévellec et al. (2010), in which a non-eddy-resolving model is used with constant isopycnal diffusivity and the only prognostic equations used are for temperature and salinity, which is comparable with the model configuration implemented in this thesis (Chapter 3). Sévellec et al. (2010) show that with increasing isopycnal diffusivity, the residual meridional overturning circulation decreases.

1.4 Isopycnal diffusivity in models

Mesoscale eddies play an important role in the energy cycle of the ocean. However, eddies are not resolved or only partially resolved in OGCMs or climate models and hence the representation of eddy effects in models relies on their parameterizations. One of the important effects of eddies is the isopycnal mixing, which can be further separated into the advective and diffusive effects of the eddies. The diffusive effect of the eddies, represented by isopycnal diffusivity, is often not resolved and its representation in models can be tricky.

Different choices of isopycnal diffusivity, also called thickness diffusivity, can be used to represent the diffusive effect of eddies in a non-eddy-resolving model. The simplest choice of isopycnal diffusivity is to use a constant value. In most non-eddy-resolving ocean models, a constant isopycnal diffusivity of $O(1000\ m^2s^{-1})$ is chosen, as it fits the timescale of flattening of isopycnals by baroclinic instability. However, other choices of isopycnal diffusivity take into account the variations in the diffusivity due to depth or stratification. Isopycnal diffusivity exponentially decreasing with depth $K(z) \sim e^{z/500m}$ was suggested by Danabasoglu and Mc Williams (1995). Further, isopycnal diffusivities proportional to vertically averaged horizontal stratification ($K(x, y) \sim |\nabla \bar{b}|$) (Griffies et al., 2005) or proportional to the local vertical stratification ($K(x, y, z) \sim \bar{b}_z$) (Danabasoglu and Marshall, 2007) have also been suggested. Visbeck et al. (1997) suggest a choice of isopycnal diffusivity based on dimensional analysis ($K(z) \sim L_{eddy}^2/\tau$ with Eady growth rate τ and length scale L_{eddy}). More sophisticated choices include paramterizing isopycnal diffusivity (Killworth, 1997, 2001; Canuto and Dubovikov, 2006; Eden and Greatbatch, 2008).

In this thesis, the parameterization by Eden and Greatbatch (2008) is used in the model setup. Isopycnal diffusivity based on by Eden and Greatbatch (2008) is derived from the eddy kinetic energy and the eddy length scale. The details of the parameterization and the model setup are given in Chapter 4.2 and Chapter 3.

1.5 Thesis Overview

The aim of this thesis is to investigate the sensitivity of tracer uptake and circulation to different isopycnal diffusivities and thus addresses the role of isopycnal diffusion in the tracer uptake and changes in circulation.

Chapter 2 provides the necessary theoretical background about the diffusive effect of mesoscale eddies and its formulation. Different mesoscale eddy closures and the numerical formulation of the paramteterization of eddy effects in form of isopycnal diffusion is detailed in this chapter.

Chapter 3 details the numerical model implemented in this study and the four experimental setups used with different isopycnal diffusivities: three setups with constant but different isopycnal diffusivities, and one setup with parameterized isopycnal diffusivity based on the Eden-Greatbatch closure.

Chapter 4 presents the results obtained from the four model setups with different isopycnal diffusivities. The changes in the overturning circulation, transport and uptake active and passive tracers, as well as the Eddy Kinetic Energy EKE) in different model setups is presented and discussed.

Chapter 5 summarizes the key results and conclusions based on the research undertaken in this thesis, followed by an outlook.

Chapter 2

Theoretical background

Coarse-resolution models do not resolve mesoscale eddies and therefore the effects of eddies are represented by subgrid scale parameterizations. Eddy parameterization scheme for non-eddy resolving ocean models have been developed by Gent and Mcwilliams (1990) and Gent et al. (1995). Gent and Mcwilliams (1990) proposed a parameterization for the effects of mesoscale eddies on the large-scale flow for use in ocean climate models, that advect tracers in addition to mixing them along isopycnal surfaces. The Gent-McWilliams (hereafter GM) parameterization aims to parameterise the "advective" effect of geostrophic eddies by means of "bolus velocity". The key idea behind this parameterization rearrange fluid parcels along isopycnals, without changing the density of individual water parcel Gent and Mcwilliams (1990). Consequently, GM represents the eddy flux of a passive tracer through both a diffusion along isopycnals and an advection by an induced velocity.

The value of isopycnal thickness diffusivity (K) is chosen as $O(1000m^2s^{-1})$ in non-eddy-resolving ocean models as it fits the time-scale of flattening of the isopycnals by baroclinic instability. The EKE budget for the large-scale oceanic flow is given by:

$$\frac{\partial \bar{e}}{\partial t} + \bar{u}.\nabla\bar{e} = \bar{S} + \overline{b'w'} - \epsilon - \nabla.M \tag{2.1}$$

In equation 2.1, $\bar{e}$ is the Eddy Kinetic Energy (EKE), u as velocity is decomposed into mean (overbars) and fluctuating parts (primes) $u = \bar{u}+u^{'}$, and on right hand side of the equation, $\bar{S}$ is the energy production term which is related to the eddy momentum fluxes and describes the eddy kinetic energy (EKE) and mean kinetic energy (MKE) exchange, energy production term $\overline{b'w'}$ denotes baroclinic instability, ϵ is related to the dissipation of

EKE, and divergence of flux M, where $\nabla.M=\nabla.\overline{u'e}+\nabla.\overline{u'p'}$ contains advection of EKE by the fluctuating flow and correlations between pressure (p) and velocity fluctuations.

2.1 Eden-Greatbatch Closure

The eddy-driven advection velocity is computed as an anti-symmetric (skew) component (K_{gm}) of the isoneutral mixing operator (Griffies, 1998), which is either taken as a constant or as the prognostics of EKE closure by Eden and Greatbatch (2008). Eden and Greatbatch closure, is a parametrization for the effect of mesoscale eddies, consists of a prognostic equation for the EKE and a diagnostic relation for an eddy length scale (L). The isopycnal diffusivity (K) for the parameterized EKE is given by:

$$K = e^{0.5}L \tag{2.2}$$

$$L = min(L_{Rhi} + L_r) \tag{2.3}$$

where, the eddy length scale L is the minimum of the Rhines scale (L_{Rhi}) and the Rossby radius (L_r). The Rhines scale and the Rossby radius are defined as:

$$L_{Rhi} = \sqrt{\frac{U}{\beta}} \tag{2.4}$$

$$L_r = min\left[\frac{c_r}{|f|}, \sqrt{\frac{c_r}{2\beta}}\right] \tag{2.5}$$

where U is a characteristic eddy velocity ($U=$ $e^{-1/2}$) and $\beta=\partial f/\partial y$ in Eq. (2.4). In Eq. (2.5), c_r denotes the first baroclinic Rossby wave speed, f is the Coriolis parameter.

In summary, Eden-Greatbatch eddy closure discusses the eddy length scale parameterization which is calculated with the EKE budget, along with prognostic equation which uses buoyancy forcing, energy production terms and calculates the isopycnal diffusivity in a non-eddy-resolving ocean model. The isopycnal diffusivity is calculated as the minimum of the length scale of Rossby radius and Rhine scale in a non-eddy-resolving model.

2.2 Mesoscale eddies and isopycnal mixing tensor

Transports by mesoscale eddies in the ocean are mainly along the isopycnal direction, which does not effect the potential energy whereas mixing across isopycnal surfaces decreases the available potential energy Olbers et al. (2012). Following Olbers et al. (2012), the simplest form of a mixing tensor is given by:

$$\boldsymbol{K} = K_D + K_I \tag{2.6}$$

where $\boldsymbol{K}$ is a 3×3 mixing tensor with different diffusivities in K_D (diapycnal direction) and K_I (isopycnal direction, isotropic mixing), which take the following form:

$$K_D = \boldsymbol{K_d}\frac{\boldsymbol{ee}}{e^2} \tag{2.7}$$

$$K_I = \boldsymbol{K_i}\left(\boldsymbol{I} - \frac{\boldsymbol{ee}}{e^2}\right) \tag{2.8}$$

where, K_d is diapycnal diffusivity, K_i is isopycnal diffusivity, $\boldsymbol{I}$ is the unit tensor, $\boldsymbol{e}$ is the vector defined normal to the local neutral surface element, $\boldsymbol{ee}$ is the tensor product that can be written as:

$$\boldsymbol{ee} = \begin{pmatrix} e_1e_1 & e_1e_2 & e_1e_3 \\ e_2e_1 & e_2e_2 & e_2e_3 \\ e_3e_1 & e_3e_2 & e_3e_3 \end{pmatrix} \tag{2.9}$$

Thus, the isopycnal mixing tensor can be written as:

$$K_I = \frac{\boldsymbol{K_i}}{e^2}\begin{pmatrix} e_2^2 + e_3^2 & -e_1e_2 & -e_1e_3 \\ -e_2e_1 & e_1^2 + e_3^2 & -e_2e_3 \\ -e_3e_1 & -e_3e_2 & e_1^2 + e_2^2 \end{pmatrix} \tag{2.10}$$

since, $|e_1|$, $|e_2| << |e_3|$ due to small aspect ratio, isopycnal mixing tensor can be further computed as:

$$K_I \approx \boldsymbol{K_i} \begin{pmatrix} 1 & 0 & s_1 \\ 0 & 1 & s_2 \\ s_1 & s_2 & s_1^2 + s_2^2 \end{pmatrix} \tag{2.11}$$

where s_1 and s_2 are components of horizontal vector $\boldsymbol{s}$ = - $\boldsymbol{e}_h/e_3$. By using this approximation, the isopycnal mixing for the passive tracer T can be given as:

$$K_I.\nabla T = \boldsymbol{K_i} \begin{pmatrix} \nabla_h T + \boldsymbol{s}\partial T/\partial z \\ \boldsymbol{s}.\nabla_h T + s^2 \partial T/\partial z \end{pmatrix} \tag{2.12}$$

Chapter 3

Model and experimental setup

3.1 Model: Python Ocean Model 2.1 (pyOM 2.1)

This study uses pyOM 2.1 Eden (2016) numerical simulation, in a global non-eddy resolving configuration with a horizontal resolution of $\sim 2^\circ \times 2^\circ$ global ocean and 45 vertical levels. All variables in the model are discretized on an Arakawa C-grid where pressure p and density ρ are centered in a box, and zonal, meridional and vertical velocities are placed on the eastern, northern and upper sides of these boxes; and u-centered grid is used for the vertical coordinate in non-equidistant spatial grid. The model also uses the hydrostatic approximation.

The TKE (Turbulent Kinetic Energy) module used in the model contains everything concerning the small-scale mixing closures, the EKE (Eddy Kinetic Energy) module contains the prognostic meso-scale mixing closure by Eden and Greatbatch (2008), the IDEMIX module (Internal gravity wave Dissipation, Energy and MIX-ing) contains the IDEMIX closure for internal gravity waves (Olbers and Eden, 2013, 2017; Eden and Olbers, 2014, 2017), and the isoneutral module contains the mixing along isopycnals.

Two parameters K_{iso} and K_{gm}, are specified to parameterize the isopycnal effects on eddies. The model uses either a constant diffusivity or the meso-scale eddy mixing closure by Eden and Greatbatch (2008).

The Eden-Greatbatch parameterization (Eden and Greatbatch, 2008) has two parts, advective (eddy advection along isopycnals, K_{gm}) and diffusive part (isopycnal eddy mixing, K_{iso}). The parameterization calculates the isopycnal diffusivity K_{iso} and K_{gm} as a function of mixing length, which is calculated as the minimum of the length scales of the Rossby radius (L_{Rossby}, distance that a particle or a wave travels before being significantly affected by the Earth's rotation) and Rhines Scale (L_{Rhines}, separates motions with respect to their transport of relative or planetary vorticity). The isopycnal diffusivity calculated in the model is the product of mixing length (eddy length, L_{eddy}) and the square root of eddy kinetic energy (EKE). Numerically, K_{iso} is formulated as follows in the model, where $max(K_{gm})$ is the maximum of K_{gm}, which is set to $10^4 m^2 s^{-1}$ and L_{min} is the minimal length scale and set to L_{min}=100m.

$$K_{iso} = min(max(K_{GM}, L_{eddy} \times \sqrt{EKE}) \tag{3.1}$$

$$L_{eddy} = max(L_{min}, min(L_{Rossby}, L_{Rhines})) \tag{3.2}$$

The list of the numerical constants used in the experiments are given in Table 3.1.

Symbol	Description	Value
nx	Number of grid points in zonal (x) direction	128
ny	Number of grid points in meridional (y) direction	64
nz	Number of grid points in vertical (z) direction	45
ρ_0	Density	1024 kg m^{-3}
K_iso_steep	Lateral diffusivity for steep slopes	500 m^2 s^{-1}
sd	Parameter controlling max. allowed isopycnal slopes	0.001
sc	Parameter controlling max. allowed isopycnal slopes	0.001
A_h	Lateral viscosity	10^4 m^2 s^{-1}
AB_{eps}	Deviation from Adam-Bashforth weighting	0.1

Table 3.1: Summary of physical and computational parameters used in the numerical simulations.

3.2 Meso-scale eddy closure

Meso-scale eddy mixing is implemented by along-isopycnal mixing and an additional eddy- driven advection velocity for tracer (Gent et al., 1995). Lateral mixing of the tracers along neutral surfaces follows the formulation by Griffies (1998). The evolution of a tracer is given by:

$$\frac{\partial T}{\partial t} = G_T - (A_T + M_T + \nabla.K\nabla T) \tag{3.3}$$

with,

$$K = K_{iso}\begin{pmatrix} 1 & 0 & s_x \\ 0 & 1 & s_y \\ s_x & s_y & s_x^2 + s_y^2 \end{pmatrix} + K_{gm}\begin{pmatrix} 0 & 0 & -s_x \\ 0 & 0 & -s_y \\ s_x & s_y & 0 \end{pmatrix} \tag{3.4}$$

where, G_T is the source and sink of tracer, A_T is the advection with the mean flow, M_T is related to the vertical mixing, and the isopycnal diffusion operator $\nabla.K\nabla T$. With isopycnal slopes s_x = - $\partial_x\rho/\partial_z\rho$ and s_y = - $\partial_y\rho/\partial_z\rho$.

The isopycnal mixing part can be treated as for horizontal fluxes and vertical mixing. This also holds for the skew diffusion. The discrete functional for the flux $K\nabla T$ by Griffies (1998) is used for isopycnal mixing and skew diffusion. The GM part can also be written as:

$$B = \begin{pmatrix} -K_{gm}s_y \\ K_{gm}s_x \\ 0 \end{pmatrix} \tag{3.5}$$

and

$$\nabla \times B = \begin{pmatrix} -\partial_z K_{gm}s_x \\ -\partial_z K_{gm}s_y \\ \partial_x K_{gm}s_x + -\partial_y K_{gm}s_y \end{pmatrix} \tag{3.6}$$

In case of too steep slopes s of the neutral surfaces, the mixing scheme by Griffies (1998) becomes unstable. Therefore the isoneutral diffusivity is multiplied by the factor d_{taper} which is given by:

$$d_{taper} = \frac{1}{2}(1 + tanh((s_c - \mid x \mid)/s_d)) \tag{3.7}$$

where s_c and s_d are parameters controlling maximum allowed isopycnal slopes. In the model configuration $s_c = 0.001$ and $s_d = 0.001$. In regions with too steep isopycnal slopes, isopycnal mixing is replaced by lateral mixing with a prescribed constant diffusivity of $Kiso_{steep} = 500\ m^2 s^{-1}$, multiplied with (1 - d_{taper}).

3.2.1 Surface forcing

The model is forced at the surface with momentum, heat, and freshwater fluxes. The forcing for the temperature T_{forc} and salinity S_{forc} is computed following in the model:

$$T_{forc} = qqnet + qqnec \times (T_0 - T) \tag{3.8}$$

and

$$S_{forc} = S_0 - S \tag{3.9}$$

where, *qqnet* and *qqnec* are the restoring forces used in the model.

In the model simulation, the movement of the active tracer is in upward direction as the diffusion is process that takes place from higher concentration to lower concentration, so for the slopes of the isopycnals and isotherms, and isopycnals and isohalines which is discussed in the section 4.1.2 and explained with figure **??**. Further in the model, the slopes of the isopycnals and isotherms are almost aligned with each other, whereas the slopes are less aligned in isopycnals and isohalines in fact more tilted. This can be understood with the two sketches shown 3.1 below:

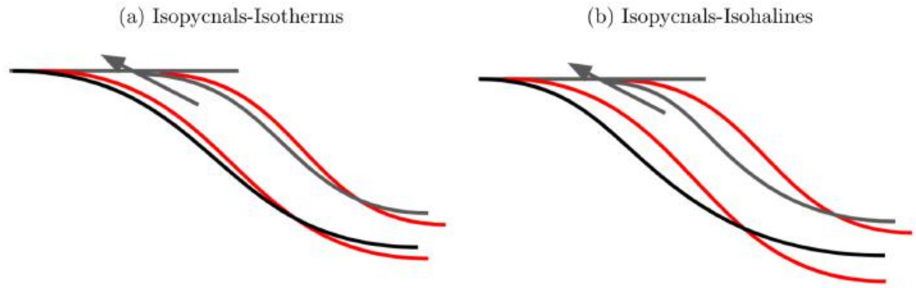

Figure 3.1: Sketch of isotherms along (a) isopycnals-isotherms, and (b) isopycnals-isohalines. Black curve shows the isopycnals and the red curve refers to isotherms in (a) and to isohalines in (b). The arrow head shows the movement of the active tracers.

3.3 Experimental setups

In this study four experiments setups have been used, which are documented in table 3.2. The first setup EG (Eden-Greatbatch setup) uses the Eden-Greatbatch eddy closure, in this the advective (K_{GM}) and diffusive (K_{iso}) part is calculated as the function of mixing length and Eddy Kinetic Energy (EKE). Advective ($K_{GM} = 1000\ m^2s^{-1}$) and diffusive parts in the second, third, and fourth setups are set to constant to 1000 m^2s^{-1}, 2000 m^2s^{-1}, and 5000 m^2s^{-1} respectively for K_{1000}, K_{2000} and K_{5000} .

Each setup was run for about 2000 years so that all the setups attain the steady state. After all the setups reach steady state, the passive tracers viz., age tracer, CFC-11 and CFC-12 are introduced in all the setups.

Model setup	K_{iso} (m^2s^{-1})	K_{GM} (m^2s^{-1})
EG	$min(\sqrt{EKE} \times L_{eddy})$	$min(\sqrt{EKE} \times L_{eddy})$
K_{1000}	1000	1000
K_{2000}	2000	1000
K_{5000}	5000	1000

Table 3.2: Model parameters for the different model setups with constant and parameterized isopycnal diffusivities.

Chapter 4

Results

In this chapter, the results from the four model setups: K_{1000}, K_{2000}, K_{5000}, and EG are discussed. The setups K_{1000}, K_{2000}, and K_{5000} have a constant isopycnal diffusivity of 1000 m^2/s, 2000 m^2/s , and 5000 m^2/s respectively, while the setup EG has an isopycnal diffusivity parameterized using the Eden-Greatbatch mesoscale eddy closure, as described in Chapter 4.2 and 3. In the first part of the chapter, the results from the setups K_{1000}, K_{2000}, and K_{5000} with respect to the circulation, active and passive tracers, and eddy energy are compared and discussed (Section 4.1). In the later part of the chapter a comparison of the results from the setups EG and K_{1000} is considered (Section 4.2).

4.1 Setups with constant isopycnal diffusivities: K_{1000}, K_{2000}, and K_{5000}

Firstly, changes in the volume transport associated with the meridional overturning circulation (MOC) and Antarctic Circumpolar Current (ACC) for the three setups are considered (Section 4.1.1). The residual overturning of the above enlisted setups with constant isopycnal diffusivity are studied in detail first and a decrease in the residual overturning has been documented with increasing isopycnal diffusivity. Thereafter, the impact of changing isopycnal diffusivity on the transport of active tracers, i.e. temperature and salinity is discussed (Section 4.1.2). The surface fluxes of temperature and salinity are discussed in Section 4.1.3, which help to explain the freshening and cooling concepts, and the changes in the MOC with increasing isopycnal diffusivity.

Passive tracers, namely age tracer, CFC-11, and CFC-12 are also introduced in the model, and the changes in the uptake of these passive tracers (and also the ocean ventilation) with different isopycnal diffusivities is documented in 4.1.4. The impact of changing isopycnal diffusivity on the Gent-McWilliams overturning and the Eddy Kinetic Energy (EKE) are discussed at the end of this section (4.1.5).

4.1.1 Circulation

The residual overturning circulation of K_{1000}, K_{2000}, and K_{5000} upto 3000 m depth are shown in figure Fig. 4.1 and the volume transport associated with the Antarctic Circumpolar Current (ACC) is shown in Fig. 4.2. As seen in the figure, strength of the circulation becomes weaker with increasing isopycnal diffusivity, from K_{1000} to K_{5000}. The volume transport for the different model setups is tabulated in Table 4.1 for the North Atlantic (NA) cell, the Southern Ocean (SO) cell, and the ACC. The NA cell is located between 30°N to 60°N whereas the SO cell is located between 40°S to 80°S. The results from the setup EG are discussed later (4.2.2).

The results of the changing isopycnal diffusivities show that the volume transport in North Atlantic decreases from $21.41 Sv$ in K_{1000}, to $19.64 Sv$ in K_{2000} and $14.54 Sv$ in K_{5000}. In the Southern Ocean the volume transport decreases from $30.42 Sv$ in K_{1000}, to $29.84 Sv$ in K_{2000} and $29.12 Sv$ in K_{5000}. The transport through Drake Passage in the ACC decreases from $141.20 Sv$ in K_{1000}, to $130.90 Sv$ in K_{2000} and $102.50 Sv$ in K_{5000}.

Further, the volume transport associated with the Antarctic Circumpolar Current (ACC), (figure Fig. 4.2) also shows a decrease in the volume transport across ACC with increasing isopycnal diffusivity. This decrease can be explained with the weakening of the Atlantic Meridional Overturning Circulation (AMOC), in which the formation of North Atlantic Deep Water (NADW) decreases and the Atlantic basin almost gets filled with the Antarctic Intermediate Water (AAIW) and Antarctic Bottom Water (AABW). The decrease in the formation of the NADW, or in other words weakening of the NADW, leads to a weaker transport in the deeper depths of the Atlantic resulting in a weaker AMOC. The reasons for the weakening of the AMOC can be understood more clearly with the active tracers (temperature and salinity) and the surfaces fluxes, which are discussed in the next sections.

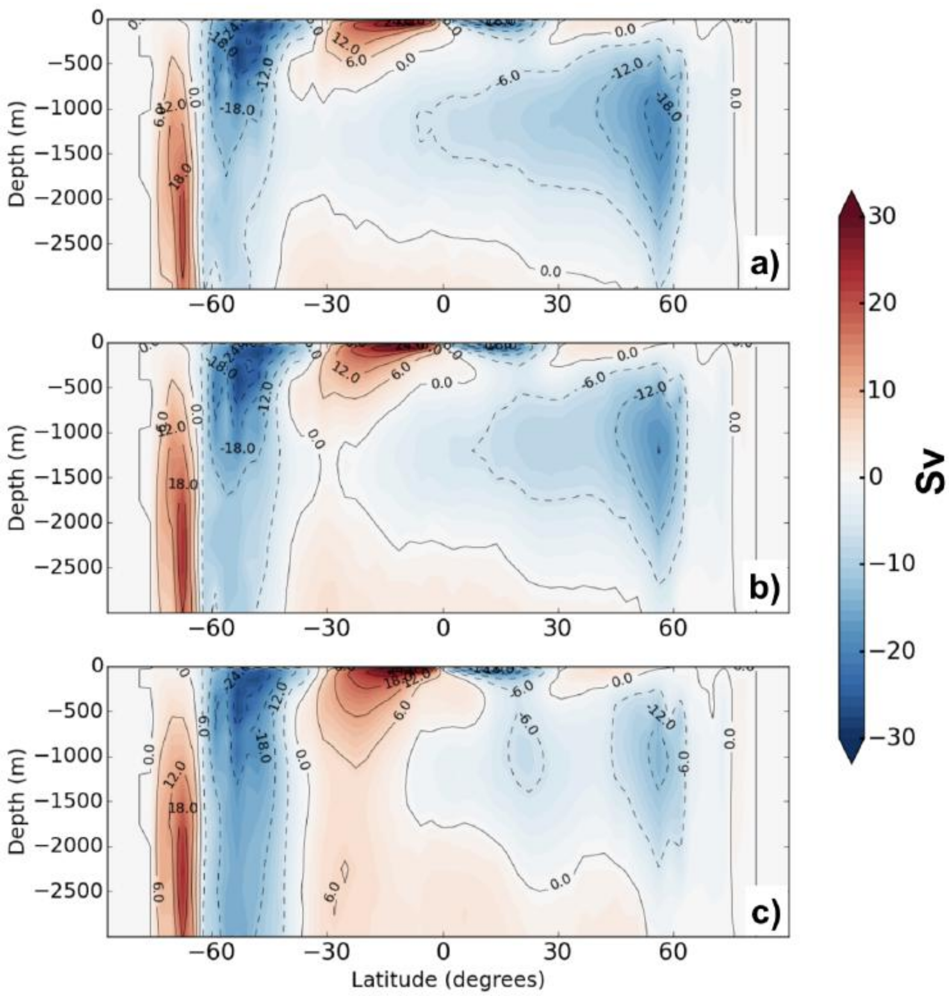

Figure 4.1: Residual overturning in Sverdrup (Sv) in the three model setups with constant isopycnal diffusivities: (a) $K_1$000, (b) K_{2000}, and (c) K_{5000}. The color shading indicates the overall volume transport in Sverdrup (Sv) with overlaid black contours indicating the same. The y-axis indicates the depth in meters and the x-axis indicates the latitude in degrees. The transport is in clockwise direction for negative contours and in anti-clockwise direction for the positive contours.

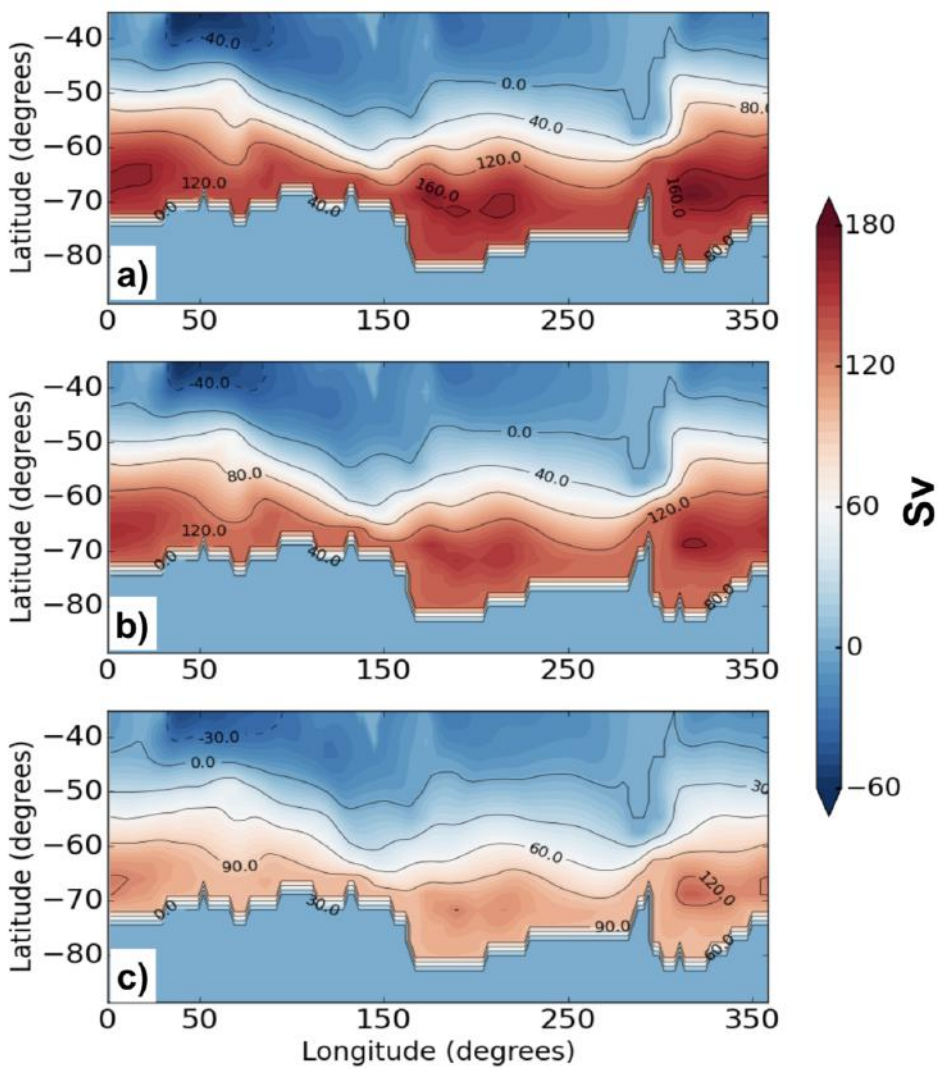

Figure 4.2: Volume transport in Sverdrup (Sv) across the Antarctic Circumpolar Current (ACC) (through Drake passage) in three model setups with constant isopycnal diffusivities: (a) K_1000, (b) K_{2000}, and (c) K_{5000}. The color shading indicates the meridional volume transport in Sverdrup (Sv) with overlaid black contours also indicating the same. The x-axis and y-axis indicate the latitude and longitude in degrees.

4.1.2 Active Tracers: Temperature and Salinity

An active tracer is a fluid property that not only gets advected by the flow but also changes the properties of the fluid itself, thus altering the flow dynamics. The active tracers in the oceanic flow discussed here are temperature and salinity, which together determine the density of the flow. The effect of different isopycnal diffusivities on temperature and salinity is assessed for the global ocean as well as for the Atlantic and Pacific ocean basins.

Model setups	Volume transport in Sverdrup (Sv)		
	North Atlantic	Southern Ocean	ACC
K_{1000}	21.41	30.42	141.20
K_{2000}	19.64	29.84	130.90
K_{5000}	14.54	29.12	102.50
EG	23.47	28.46	163.80

Table 4.1: The volume transport in the North Atlantic (NA) cell, Southern Ocean (SO) cell and in the Antarctic Circumpolar Current (ACC) (through Drake Passage) in Sverdrup Sv for all the model setups.

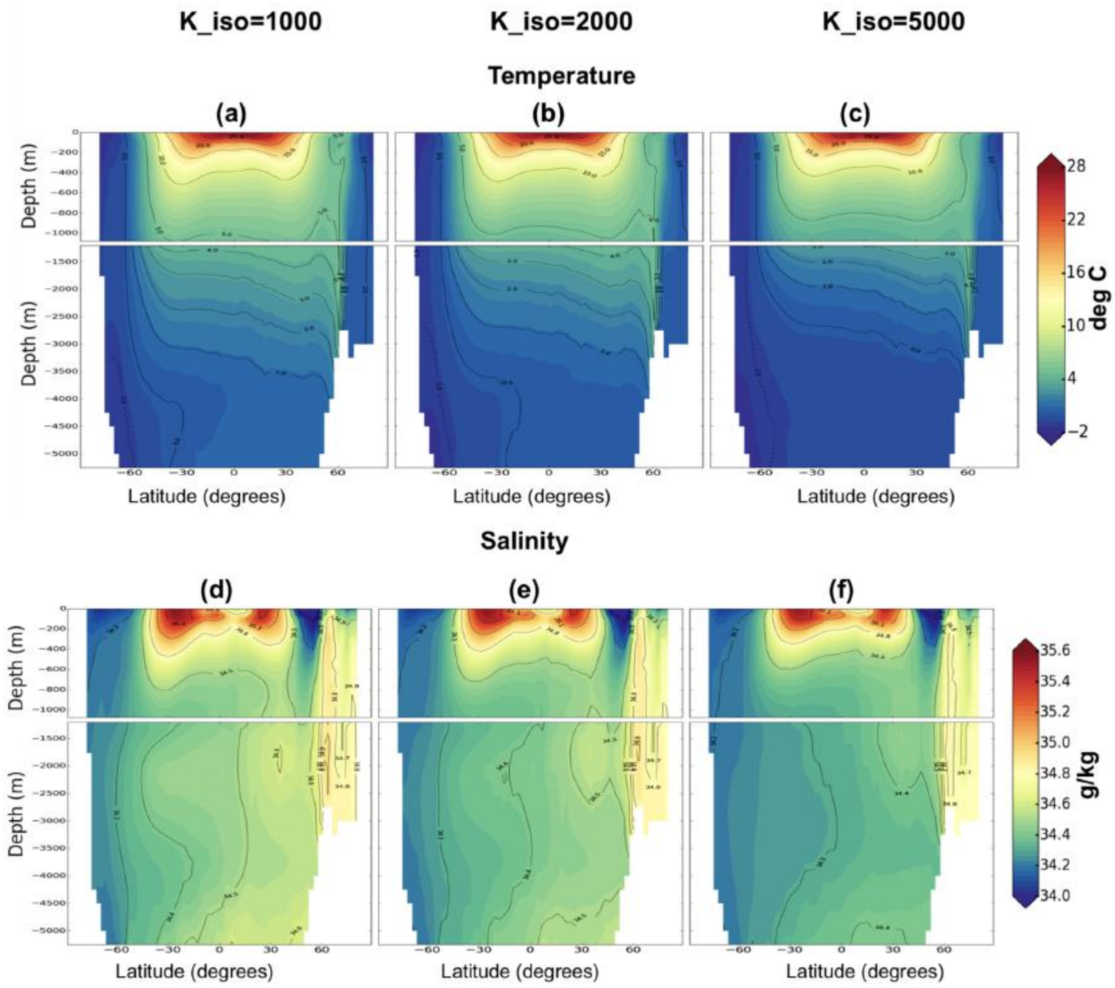

Figure 4.3: Zonally averaged latitude-depth sections of temperature and salinity for model setups (a,d) K_{1000}, (b,e) K_{2000}, and (c,f) K_{5000}. The upper panels in each subplot indicate the temperature (a-c) (and salinity (d-f)) in the upper 1000 m and the lower panels indicate temperature (a-c) (and salinity (d-f)) in the interior and deep ocean. The color shading indicates (a-c)temperature (°C) and (d-f) salinity (g/kg) with overlaid black contours indicating the isotherms and isohalines respectively. The x-axis indicates latitude in degrees and the y-axis indicates depth in meters.

The zonally averaged latitude-depth sections of temperature and salinity for three experimental setups with constant isopycnal diffusivities K_{1000}, K_{2000} and K_{5000} are shown in Fig. 4.3. The figures clearly indicate that the interior of the ocean is getting colder and fresher with increasing isopycnal diffusivity. Further, the globally averaged depth profiles of temperature and salinity are shown in Fig. 4.4, where the increasing isopycnal diffusivity leads to cooling and freshening respectively, the effect being more prominent in the interior and the deep ocean. To look more closely into the individual oceanic basins, the temperature and salinity depth profiles for the Pacific and Atlantic ocean is shown in figure Fig. 4.5. In both the ocean basins, the cooling and freshening in the interior with increasing isopycnal diffusivity is similar to the global ocean, however the extent of cooling and freshening in both the basins differs. For instance, at an intermediate depth (about 2000 m), the cooling and freshening between the setups K_{5000} and K_{1000} is more pronounced for the Atlantic than it is for the Pacific.

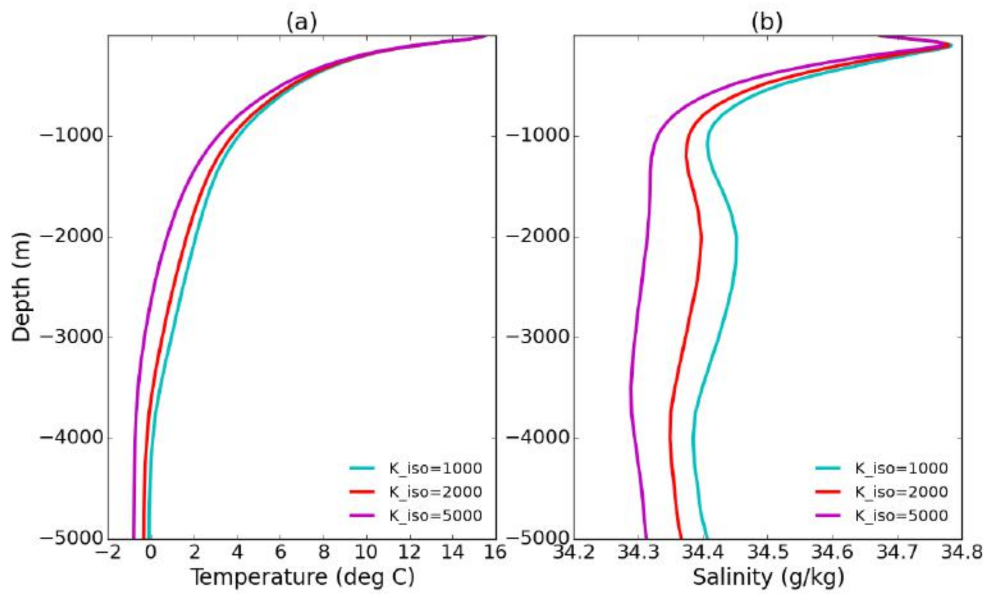

Figure 4.4: Globally averaged profiles of (a) temperature and (b) salinity. The different colors indicate different model setups: (cyan) K_{1000}, (red) K_{2000}, and (magenta) K_{5000}. Note that the x-axis is temperature in °C in (a) and salinity in g/kg in (b).

These changes in temperature and salinity in turn affect the deep watermasses in the Atlantic ocean, i.e. the North Atlantic Deep Water (NADW) formed between 1500 and 4000 m depth, which becomes significantly cooler and fresher between the setups K_{5000} and K_{1000}, as seen in Fig. 4.5. In the Southern Ocean, the Antarctic Intermediate Water

(AAIW) (at about 700-1200 m depth) and Antarctic Bottom Water (AABW) (below 4000 m depth) also become colder and fresher with the increasing isopycnal diffusivity, as seen in Fig. 4.3, as well as in Fig. 4.6 which shows the zonally averaged isotherms, isohalines, and isopycnals.

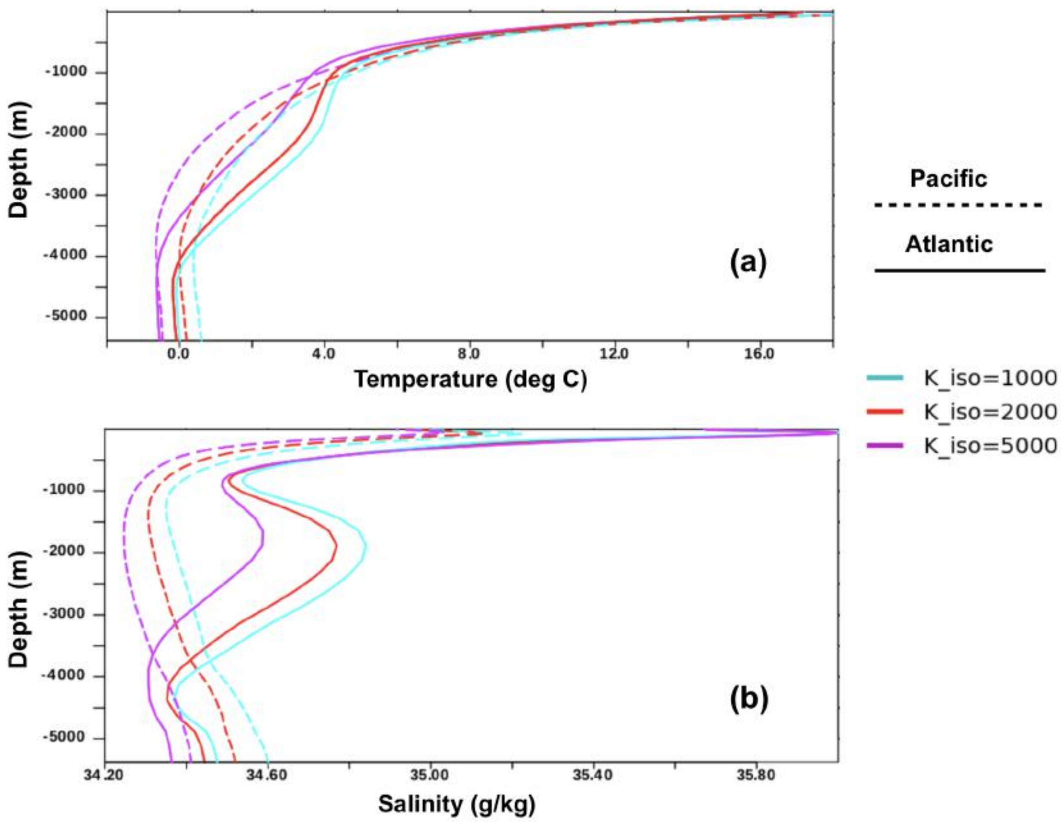

Figure 4.5: Zonally and meridionally averaged profiles of (a) temperature and (b) salinity for the Atlantic and Pacific oceans. The different colors indicate different model setups: (cyan) K_{1000}, (red) K_{2000}, and (magenta) K_{5000}. The solid lines represent the Atlantic and the dashed lines represent the Pacific ocean. Note that the x-axis is temperature in °C in (a) and salinity in g/kg in (b).

The reason for this cooling and freshening effect can be understood with the outcropping of the slopes of isotherms and isohalines along the isopycnals in the upward direction, i.e. the direction of the movement of the tracer is from higher concentration to lower concentration, as seen in Fig. 4.6. From the figure it can be clearly accounted that the freshening in the ocean is stronger (because the slopes of isopycnals are not aligned with the isohalines, thus affecting more tracer diffusion) than the cooling (because the slopes of isopycnals are almost aligned with isotherms).

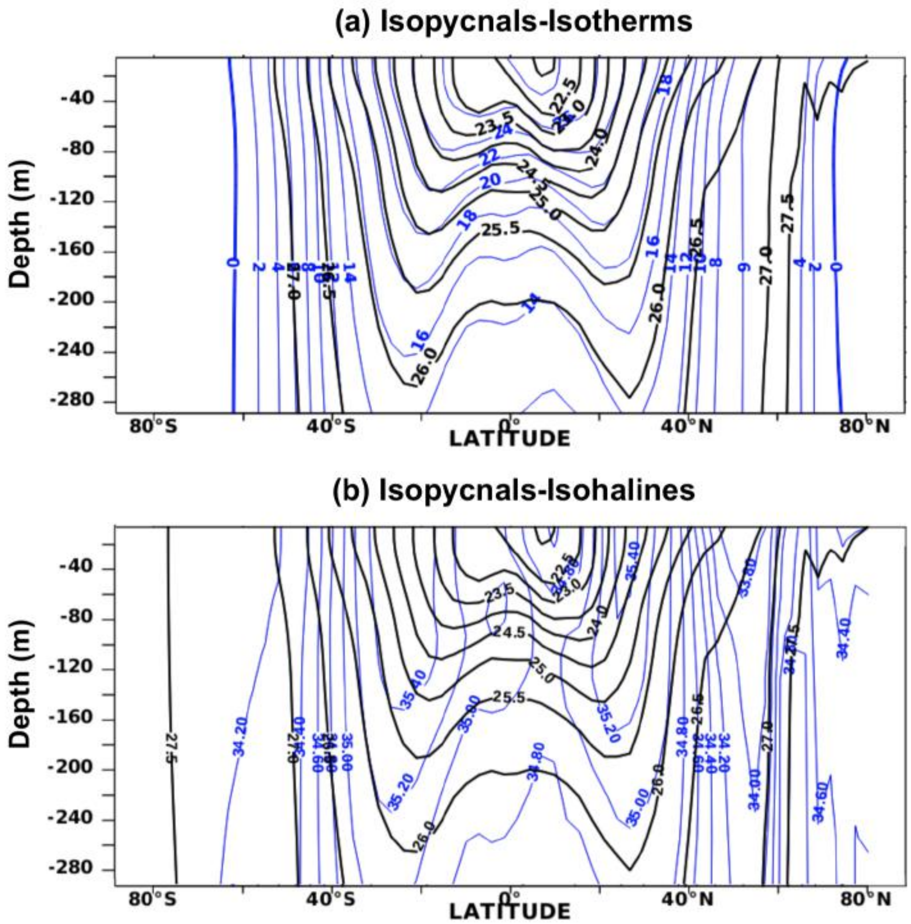

Figure 4.6: Zonally averaged (a) isotherms-isopycnals and (b) isohalines-isopycnals in the upper 300 m shown for the model setup K_{1000}. Black lines indicate isopycnals, blue lines indicate isotherms in (a) and isohalines in (b). The x-axis is temperature is latitude in degrees and y-axis is depth in meters. The results for K_{2000} and K_{5000}, not shown here, are qualitatively similar.

4.1.3 Surface fluxes of heat and freshwater

To further understand the temperature and salinity changes in the interior and deep ocean seen in the previous figures, the effect of changing isopycnal diffusivity on the surface fluxes heat and freshwater are examined. Surface fluxes of temperature and salinity are shown in figure Fig. 4.7, which are averaged zonally over the global ocean for the three model setups: K_{1000} , K_{2000} and K_{5000}.

The freshwater flux, or the salt flux, is calculated from the difference between evaporation and precipitation. A negative salt flux indicates that the ocean surface gains freshwater thus making the seawater fresher, while a positive flux indicates that the seawater is saltier.

A negative temperature flux indicates that the ocean surface gains heat thus making the seawater warmer, while a positive flux indicates cooling of the sea surface.

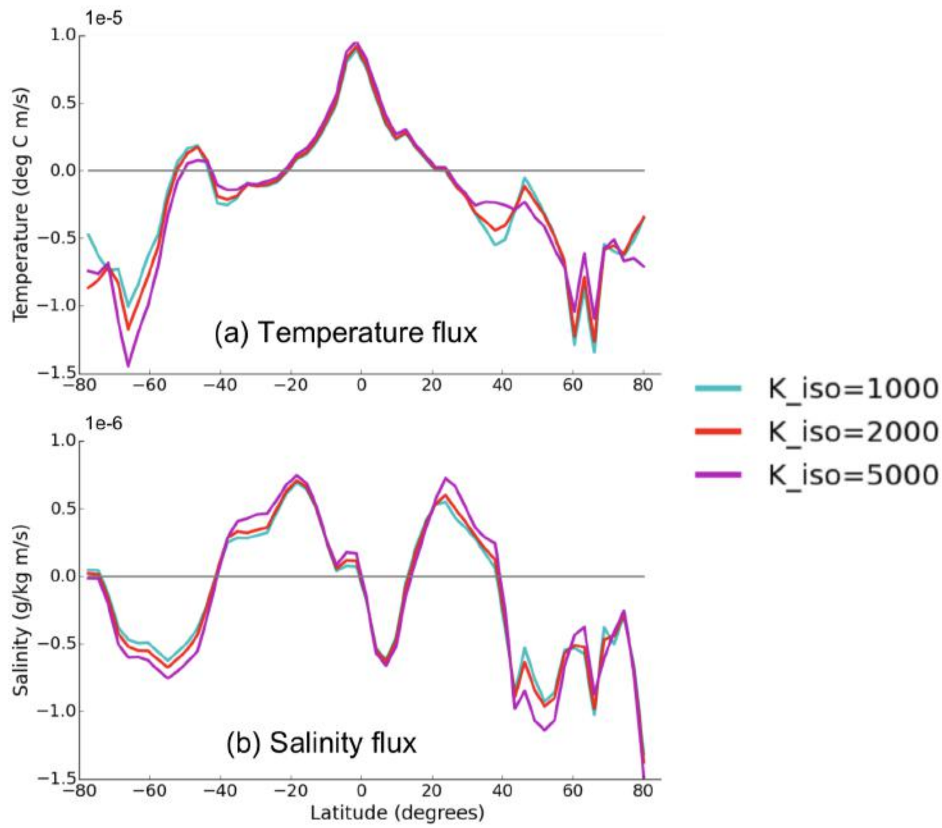

Figure 4.7: Surface fluxes of (a) temperature and (b) salinity. The different colors indicate different model setups: (cyan) K_{1000}, (red) K_{2000}, and (magenta) K_{5000}. Note that the x-axis is temperature flux in °C m/s in (a) and salinity in $g/kg\ m/s$ in (b).

At higher latitudes, signature of relatively more freshening and cooling with increasing isopycnal diffusivity is seen. However, the differences in the temperature and salt fluxes in the three model setups show negligible differences at the equator. This freshening and cooling is also seen in Fig. 4.3, in which near the equator there is less warming and more freshening and at higher latitudes cooling and freshening complement each other. In fact, the increased freshening of ocean interior is not only seen in the surface fluxes but also in figures Fig. 4.3, Fig. 4.4, Fig. 4.5, and Fig. 4.6.

Thus, active tracers and surface fluxes all together explain the reason for the weakening of the meridional overturning circulation (MOC) and Antarctic Circumpolar Current

(ACC) with increasing isopycnal diffusivity, as discussed in the previous section.

4.1.4 Passive Tracers: Age tracer and CFC-11

Passive tracers, unlike active tracers, have no influence on the flow. Passive tracers can thus be effectively used to understand the advective and diffusive processes in a flow without changes in the properties of the flow itself by the tracer. Three passive tracers are used in this study, namely age tracer, CFC-11, and CFC-12. CFC-11 and CFC-12 are of anthropogenic origin that have been introduced into the atmosphere by human activities and their concentrations have increased from zero since 1930s.

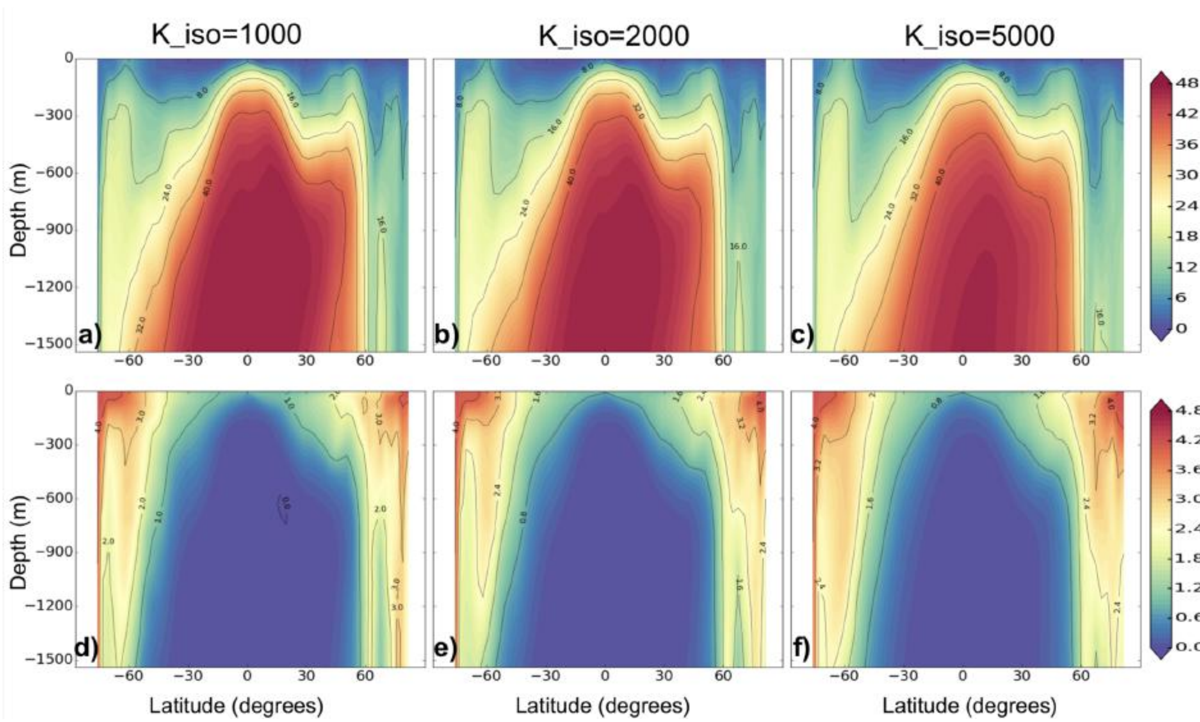

Figure 4.8: Zonally averaged latitude-depth sections of the passive tracers in the upper 1500 m depth for model setups (a) K_{1000}, (b) K_{2000}, and (c) K_{5000}. Age tracer (in years) is shown in the upper panel (a, b, c) and CFC-11 (in pptv) is shown in the lower panel (d, e, f).

In the numerical simulations, these passive tracers are simulated from beginning of 1931 with zero concentrations in the atmosphere and have been increased till 1977 and are conserved in the ocean. In this way, 48 years of data for the passive tracers is taken into account. All the passive tracers are introduced to all the setups after the model has attained a state of equilibrium. The results from the age tracer and CFC-11 are considered, whereas the results from CFC-12 are not shown because the conclusions are qualitatively similar to the ones for CFC-11.

Zonally averaged distribution of the age tracer and CFC-11 for three model setups with different isopycnal diffusivities K_{1000} , K_{2000} and K_{5000} are shown for upper 1500 m in Fig. 4.8. The regions of older ages for the age tracer coincide with higher concentrations of CFC-11, indicating that a younger watermass has a higher concentration of CFC-11. The distribution of watermass ages and CFC-11 concentrations provide information about the ventilation pathways in the ocean. They are also important to understand the storage and distribution of anthropogenic Carbon in the ocean. It can be seen clearly from the figure Fig. 4.8 that the interior of the ocean is getting more ventilated with the increasing isopycnal diffusivity. The distribution of the age tracer indicates that the interior of the ocean is getting younger. Similar effect can be seen from the distribution of CFC-11, with increasing isopycnal diffusivity the uptake of the tracer is enhanced thus ventilating the ocean interior.

4.1.5 Impact on GM Overturning and EKE

The GM parameterization, as discussed in Chapter 4, aims to parameterize the advective effect of mesoscale eddies by means of a bolus velocity, B. This bolus velocity B is directly related to the slope of isopycnals (cf. Eq. (3.5)). The results so far show that the slope of isopycnals decreases with increasing isopycnal diffusivity. So, the feedback on GM parameterization is expected (cf. Eq. (3.5)). The meridional component of the GM streamfunction for the three setups K_{1000} , K_{2000} and K_{5000} in the upper 3000 m depth is shown in figure Fig. 4.9. As expected, with increasing isopycnal diffusivity there is a decrease in the meridional GM component, owing to the decrease in isopycnal slopes. The difference in the meridional or the bolus streamfunction between K_{1000} and K_{5000} appears relatively larger in the Southern Ocean and than it is for the North Atlantic.

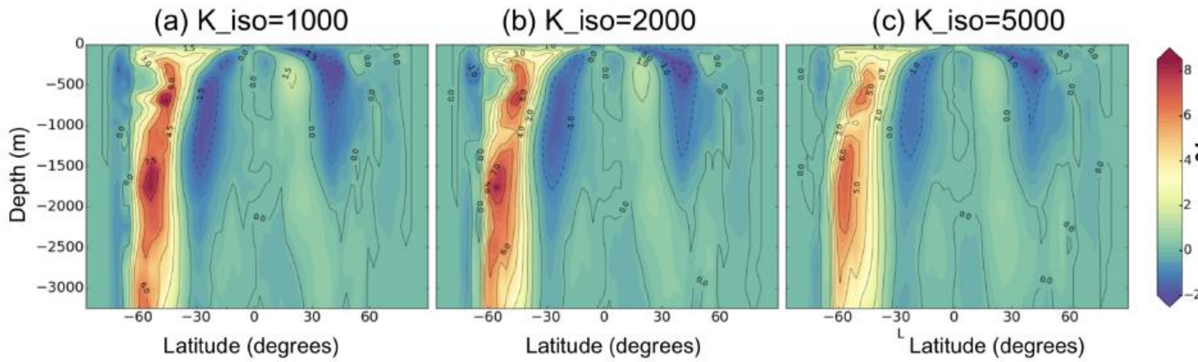

Figure 4.9: Meridional component of the GM streamfunction in the upper 3000 m depth in three model setups: (a) K_1000, (b) K_{2000}, and (c) K_{5000}. The color shading indicates the bolus depth in m^3/s with overlaid black contours indicating the same. The y-axis indicates the depth in meters and the x-axis indicates the latitude in degrees.

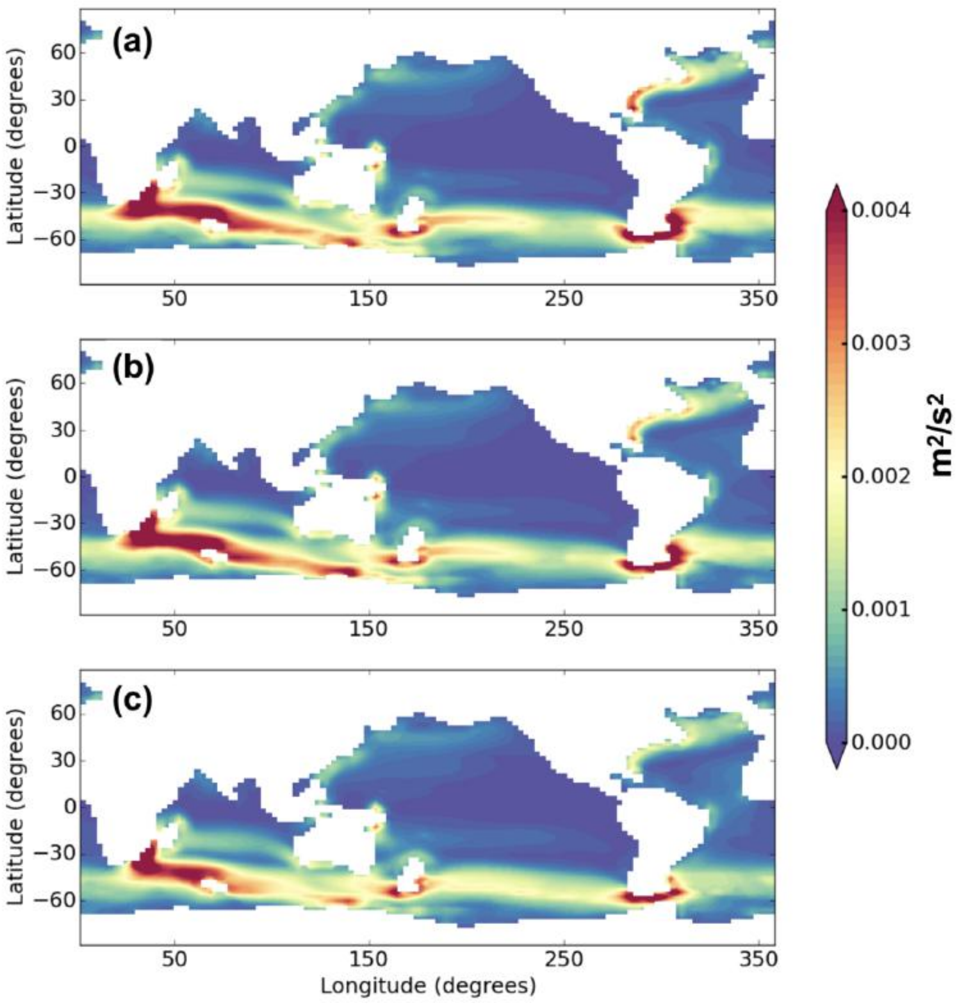

Figure 4.10: Eddy Kinetic Energy (EKE) at a depth of 1000m in the three model setups: (a) K_1000, (b) K_{2000}, and (c) K_{5000}. The color shading indicates EKE in m^2/s^2. The x-axis and y-axis indicate longitude and latitude in degrees.

Further, the effects of changing isopycnal diffusivity on EKE is considered. The eddy energy production is related to baroclinic instability as follows:

$$\overline{b'w'} = K\frac{|\nabla_h \bar{b}|^2}{N^2} \tag{4.1}$$

The relation of the baroclinic production term $\overline{b'w'}$ in Eq. (4.1) with the energy production (Eq. (4.1) R.H.S) involves the factor K. EKE for the three model setups K_{1000} , K_{2000} and K_{5000} at a depth of 1000m is shown in Fig. 4.10. In general, the EKE decreases with increasing isopycnal diffusivity. In particular, the EKE decreases significantly near the western boundaries (e.g. the Gulf Stream and the Kuroshio systems), in the Southern Ocean and in the North Atlantic.

This decrease in the EKE can be explained by Eq. (4.1). As the isopycnal slopes become less steeper with increasing isopycnal diffusivity, there is a reduction in the baroclinic production term, in turn resulting in a reduction in the the total energy of the system, and therefore also a decrease in the EKE.

4.2 Parameterized vs. Constant Isopycnal Diffusivity: EG vs K_{1000}

In the Eden-Greatbatch parameterization based on (Eden and Greatbatch, 2008), as discussed in Chapter , isopycnal diffusivity is calculated as the function of the EKE and the mixing length. This parameterized isopycnal diffusivity is implemented in the model setup EG where the isopycnal diffusivity varies spatially, rather than being constant everywhere as in the model setups K_{1000} , K_{2000} and K_{5000} discussed so far. A comparison between a constant and a spatially varying paramterized isopycnal diffusivity and their effects are elaborated in this section.

In this section, the effects of different isopycnal diffusivities on the circulation, EKE, and the transport of active and passive tracers is compared between the setups EG and K_{1000}. Note that, unlike the K_{1000} setup where both advective (K_{gm}) and diffusive terms (K_{iso}) are constant (1000 m^2s^{-1}), in the EG setup both the advective (K_{gm}) and diffusive terms (K_{iso}) are calculated from the mixing length theory in the model. Since, an isopycnal diffusivity of $O(1000\ m^2s^{-1})$ fits the timescale of flattening of isopycnals by baroclinic instability, this value of isopycnal diffusivity is used in most non-eddy-resolving ocean models. Thus the choice of setup K_{1000}, with a constant isopycnal diffusivity of 1000 m^2s^{-1}, appears to be an appropriate choice for comparison with the EG setup.

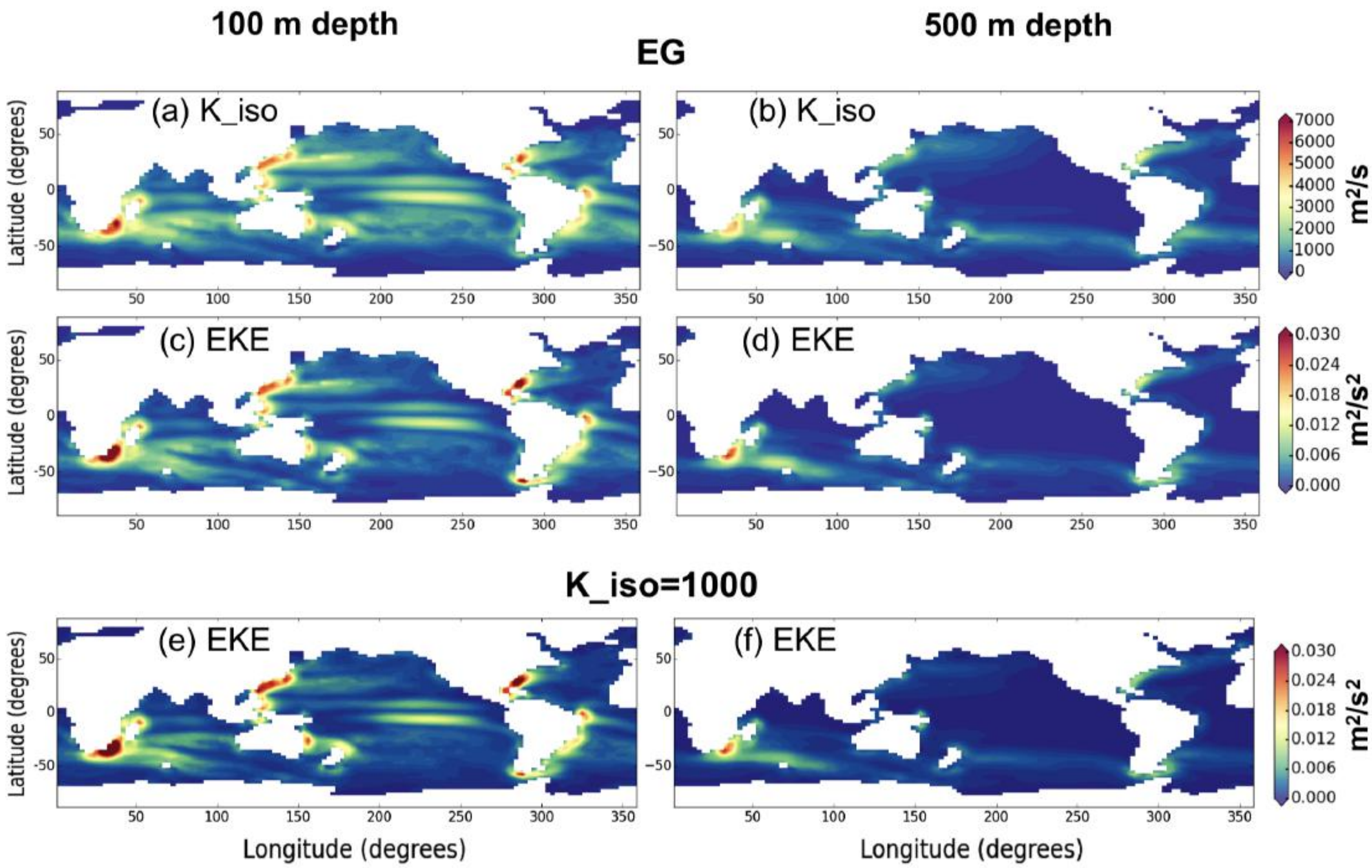

Figure 4.11: Eddy Kinetic Energy (EKE) (in m^2/s^2) at depths of 100m and 500m compared for the setups (c-d) EG and (e-f) K_{1000}. For the model setup EG, (a-b) isopycnal diffusivities (in m^2/s) are also shown at 100m and 500m depths. In all subplots, the x-axis and y-axis indicate longitude and latitude in degrees.

4.2.1 Isopycnal Diffusivity and EKE

For the EG setup, isopycnal diffusivity and EKE at depths of 100m and 500m are shown in Fig. 4.11. For the same depths, the EKE from the setup K_{1000} is also compared with the EKE from the EG setup Fig. 4.11(e-f).

Firstly, the parameterized EG isopycnal diffusivity (Fig. 4.11(a-b)) is spatially inhomogenous, where the western boundary current systems show strong signatures of high isopycnal diffusivities. High diffusivities are also seen in the Southern Ocean, North Atlantic and the

Pacific Ocean, but the ACC regions shows weaker diffusivity values. However, the isopycnal diffusivities decrease substantially at 500m depth than at 100m depth, although the regions of high isopycnal diffusivity at 500m depth still remain the same as at 100m depth, i.e. the western boundary current systems and the major ocean basins. In the Southern Ocean and North Atlantic, the magnitude of isopycnal diffusivity appears to be even less than (1000 m^2s^{-1}). For the EG setup the average value of isopycnal diffusivity based on the Eden-Greatbatch eddy closure is 241.1 m^2s^{-1}.

The isopycnal diffusivities effect the EKE, which can also be seen for the setup EG in Fig. 4.11(c-d) and for the setup K_{1000} in Fig. 4.11(e-f) at depths of 100m and 500m. In the setup EG, for both 100m and 500m depths the regions of high EKE coincide with the regions of high isopycnal diffusivties, which is no surprise since K_{iso} in this setup is derived from the EKE. On the other hand, in the setup K_{1000} (with a constant K_{iso}), the regions of high EKE are fairly similar to the EKE in setup EG in regions such as the western boundary current systems and the major ocean basins, but in regions such as the ACC the setup K_{1000} has much lower EKE than setup EG. How these differences in the isopycnal diffusivities in these two setups effect the circulation and transport is discussed in the next section.

4.2.2 Circulation

The residual overturning circulation in setups EG (Fig. 4.12a) and K_{1000} (Fig. 4.12b) upto 3000 m depth and the volume transport associated with the ACC (transport through Drake Passage) for the respective setups are shown in (Fig. 4.12c) and (Fig. 4.12d).

As seen in the figure, strength of the circulation becomes weaker with increasing isopycnal diffusivity, from K_{1000} to K_{5000}. The volume transport for both the setups is tabulated in Table 4.1 for the North Atlantic (NA) cell, the Southern Ocean (SO) cell, and the ACC. As seen in Fig. 4.12 and Table 4.1, the volume transport for the North Atlantic cell is stronger and for the Southern Ocean cell it is weaker for the EG setup than for K_{1000} setup. However, the overall volume transport increases in the EG setup, which can be seen not just in the North Atlantic Deep Water (NADW) formation (23.47 Sv) but also across the ACC (163.8 Sv), whereas in the K_{1000} setup the volume transport in the North Atlantic is 21.41 Sv and across ACC is 141.20 Sv. Therefore, a model with parameterized isopycnal diffusivity based on Eden-Greatbatch closure shows a stronger volume transport than a model with a constant value of isopycnal diffusivity.

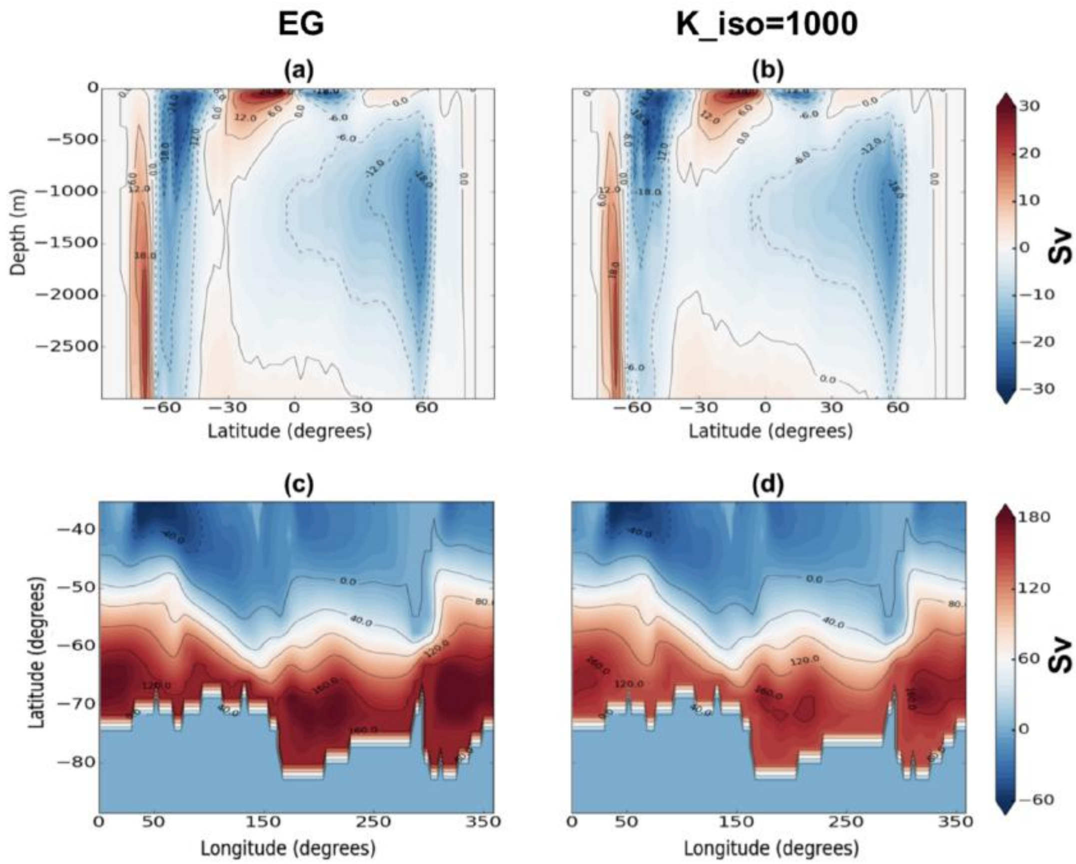

Figure 4.12: Residual overturning in the upper 3000 m (a-b) and volume transport across the Antarctic Circumpolar Current (ACC) (through Drake passage) (c-d) in the model setups EG (a and c) and (b and d) K_{1000}. The color shading indicates the overall volume transport in Sverdrup (Sv) with overlaid black contours indicating the same. In the upper panel, x-axis is latitude in degrees and y-axis is depth in meters. In the lower panel, x-axis is longitude in degrees and y-axis is latitude in degrees.

4.2.3 Active and Passive Tracers

Here the impact of different isopycnal diffusivities on the transport and uptake of active and passive tracers in the setups EG and K_{1000} are described.

Firstly, the active tracers- temperature and salinity are looked into. The zonally averaged latitude-depth sections of temperature and salinity for setups EG and K_{1000} are compared in Fig. 4.13. The oceanic interior both in the Southern Ocean and the North

Atlantic is warmer and saltier in the EG setup as compared to K_{1000} where it is relatively colder and fresher. In the setup EG, the saltier watermass in the ocean interior is a signature of NADW formation which is getting saltier. This strengthens the formation of NADW resulting in a stronger circulation in the AMOC. This is consistent with the stronger volume transport seen in the setup EG than for K_{1000}, as discussed in Section 4.2.2. This changes in temperature and salinity not only affect the NADW cell but also the global ocean circulation and the overall volume transport as discussed before.
The surface fluxes of temperature and salinity for the setups EG and K_{1000} (not shown) are fairly similar and do not show much differences.

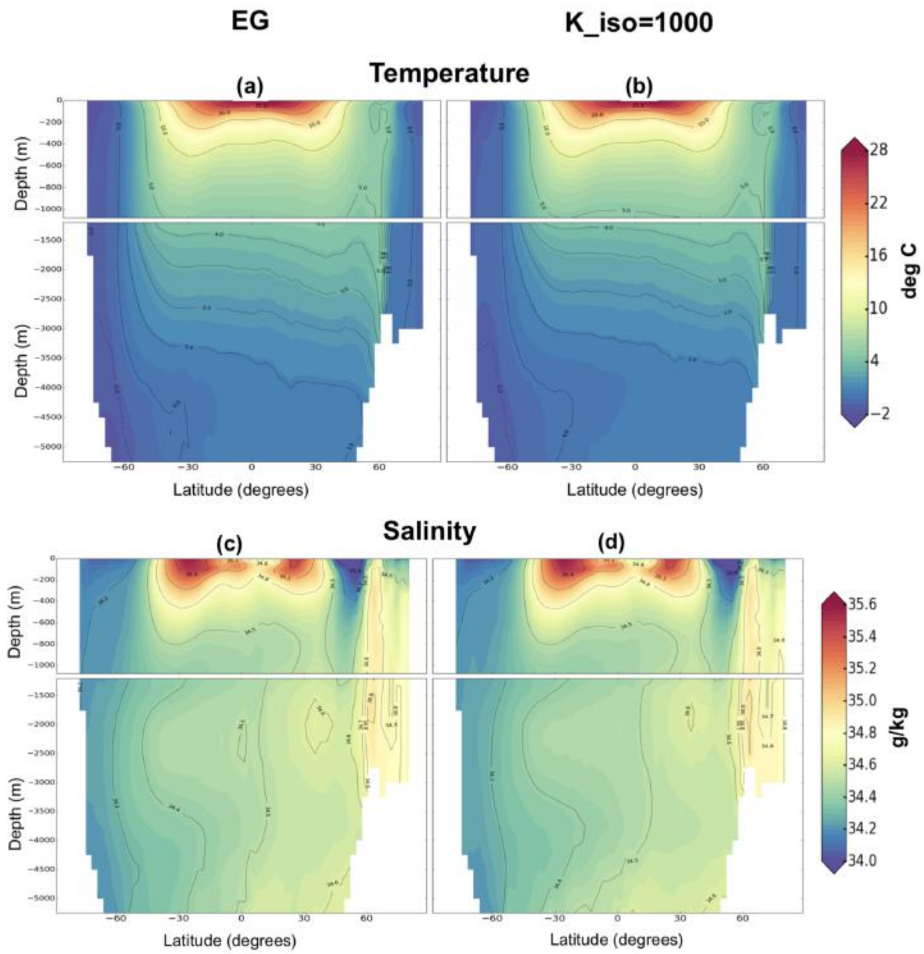

Figure 4.13: Zonally averaged latitude-depth sections of temperature and salinity for model setups (a, c) EG and (b, d) K_{1000}. The upper panels in each subplot indicate the temperature (a and b) (and salinity (c and d)) in the upper 1000 m and the lower panels indicate temperature (a and b) (and salinity (c and d)) in the interior and deep ocean. The color shading indicates (a-b)temperature (°C) and (c-d) salinity (g/kg) with overlaid black contours indicating indicating the isotherms and isohalines respectively. The x-axis indicates latitude in degrees and the y-axis indicates depth in meters.

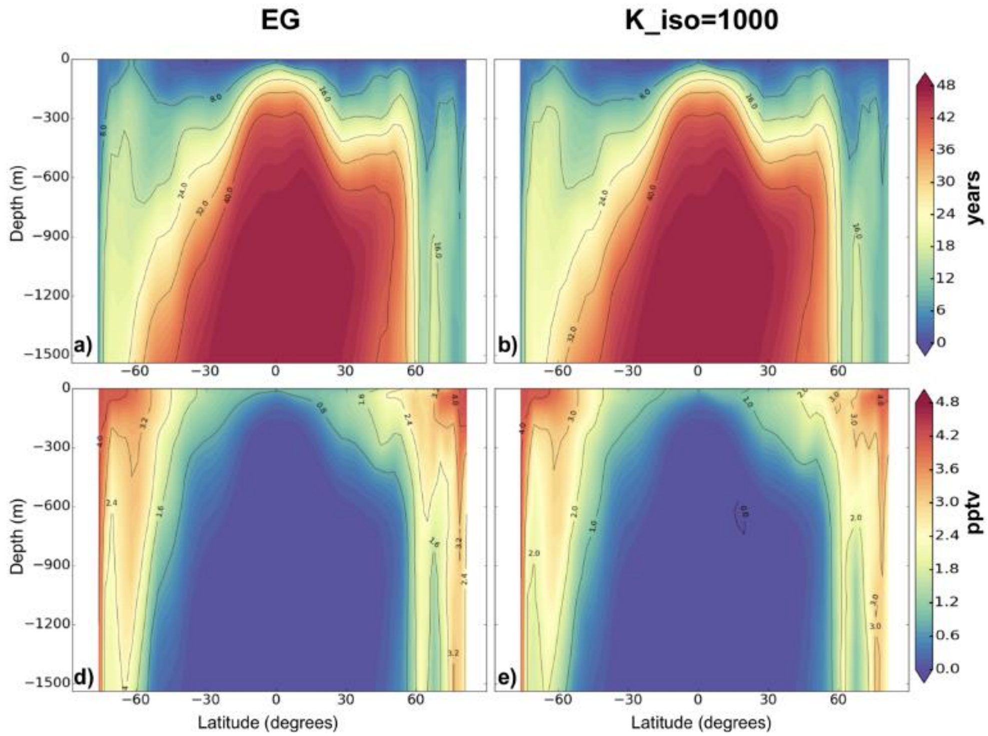

Figure 4.14: Zonally averaged latitude-depth sections of the passive tracers in the upper 1500 m depth for model setups (a) for model setups (a, c) EG and (b, d) K_{1000}. Age tracer (in years) is shown in the upper panel (a, b) and CFC-11 (in pptv) is shown in the lower panel (c, d).

The distribution and uptake of two passive tracers, age tracer and CFC-11 are compared for setup EG and K_{1000}. The tracers are introduced in the model in the same way as described in Section 4.1.4. Zonally averaged distribution of the age tracer and CFC-11 for the model setups EG (Fig. 4.14(a,c)) and K_{1000} (Fig. 4.14(b,d)) are shown for the upper 1500 m in Fig. 4.14. As seen earlier, the regions of older watermasses are the regions with higher concentrations of CFC-11. The distribution of watermass ages and CFC-11 concentrations provide information about the ventilation pathways in the ocean. It can be seen with the age tracer that the interior of the ocean is getting younger in K_{1000} setup and older in EG setup i.e., the ocean interior is getting much more ventilated in K_{1000} setup compared to EG setup. Along with this, the tracer uptake, i.e. the uptake of CFC-11, is higher in K_{1000} than in EG. In addition, the uptake is more in the Southern Ocean i.e., the water mass in Southern Ocean is getting more ventilated than the North Atlantic where the uptake is comparatively less and the water mass is older and less ventilated.

Chapter 5

Conclusions

The results obtained from the research undertaken in the thesis are compiled in this chapter. The main results are discussed followed by an outlook.

The aim of this thesis has been to investigate the changes in tracer uptake and circulation due to changing isopycnal diffusivity. To achieve this a global non-eddy resolving model configuration of the Python Ocean Model 2.1 (pyOM 2.1) is implemented with a horizontal resolution of $\sim 2° \times 2°$ (cf. Chapter 3). To assess the effects of different isopycnal diffusivities, four model setups are used with different values of isopycnal diffusivities: K_{1000}, K_{2000}, K_{5000}, and EG. The setups K_{1000}, K_{2000}, and K_{5000} have a constant value of isopycnal diffusivity viz. 1000 m^2/s, 2000 m^2/s , and 5000 m^2/s respectively. In the setup EG isopycnal diffusivity is parameterized using the Eden-Greatbatch mesosscale eddy closure (Eden and Greatbatch, 2008) (cf. Chapter 4.2). To assess the changes in tracer uptake and ocean ventilation with different isopycnal diffusivities in the four model setups, passive tracers– age tracer, CFC-11, and CFC-12 are introduced in the model and from the year 1930 and integrated in the model for 48 years.

All the model setups are run for about 2000 years, and the results presented in this thesis are analyzed from the equilibrated state of the model. The sections below summarize the key findings in the changes in the circulation, tracer uptake and transport of the active tracers (temperature and salinity) and passive tracers (age tracer and CFC-11).

5.1 Circulation

The residual overturning circulation in the four model setups shows that the volume transport in the North Atlantic (NA) cell decreases with increasing isopycnal diffusivity—from 21.41 Sv in setup K_{1000} to 14.54 Sv in setup K_{5000}, but the transport increases to 23.47 Sv in the setup EG. The volume transport through the Antarctic Circumpolar Current (ACC) (through Drake Passage) shows a similar trend: the transport decreases from 141.2 Sv in setup K_{1000} to 102.5 Sv in setup K_{5000}, but increases in the setup EG to 163.8 Sv. In the Southern Ocean (SO) cell, although the volume transport decreases with increasing isopycnal diffusivity–from 30.42 Sv in setup K_{1000} to 29.12 Sv in setup K_{5000}, the transport in the setup EG also decreases to 28.46 Sv (cf. Table 4.1). This is related to the relatively high isopycnal diffusivities in the Southern Ocean than the North Atlantic and the ACC in the EG setup Fig. 4.11.

Overall, for model setups constant isopycnal diffusivity, the overturning circulation becomes weaker in the NA and SO cell as well the ACC with increasing values of isopycnal diffusivities. As compared to other three setups, an isopycnal diffusivity based on Eden-Greatbatch closure as in setup EG shows a stronger transport in the NA cell and ACC but weaker transport in the SO cell (but still stronger transport than NA cell in the EG setup).

5.2 Active tracers: temperature and salinity

The distribution of active tracers i.e. temperature and salinity in the four model setups shows that with increasing isopycnal diffusivity in setups K_{1000} , K_{2000}, and K_{5000}, the interior of the ocean becomes colder and fresher (Fig. 4.3). This cooling and freshening in the oceanic interior is more prominent in the Atlantic Ocean–which in turn weakens the deep water formation (NADW) and thus the overturning circulation in the Atlantic basin– than it is for the Pacific Ocean (Fig. 4.5). This cooling and freshening of the ocean interior is attributed to the outcropping of the slopes of isotherms and isohalines along the isopycnals in the upward direction. The slopes of isopycnals are not aligned with the isohalines, unlike the isotherms which are aligned, leading to more tracer diffusion and hence more freshening than the cooling (Fig. 4.6). The surface fluxes of temperature and salinity also show signatures of relatively more freshening and cooling with increasing isopycnal diffusivity at higher latitudes. On the contrary, in the setup EG the oceanic interior becomes warmer and saltier than setup K_{1000}, for instance in the NA cell (Fig. 4.13). This decrease in cooling and freshening in the NA cell enhances the deep water formation, thus resulting in a stronger NA transport in the EG setup (Fig. 4.12, cf. Table 4.1).

Overall, an increasing isopycnal diffusivity acts to make the oceanic interior cooler and fresher, thus affecting the deep water formation and consequently the overturning circulation which weakens with increasing isopycnal diffusivity (in setups K_{1000} , K_{2000}, and K_{5000}). In EG setup with parameterized isopycnal diffusivity, the interior of the ocean becomes warmer and saltier, resulting in enhanced deep water formation shows and hence a stronger overturning circulation.

5.3 Passive tracers: age tracer and CFC-11

The distribution of passive tracers i.e. age tracer and CFC-11 in the four model setups shows that with increasing isopycnal diffusivity in setups K_{1000} , K_{2000}, and K_{5000}, the interior of the ocean becomes younger with low concentrations of CFC-11. This indicates that with higher isopycnal diffusivity there is a higher tracer uptake and thus the interior of the ocean is getting more ventilated (Fig. 4.8). On the other hand, for the EG setup the interior of the ocean is getting older than in the K_{1000} i.e., the tracer uptake is reduced, thus leading to less ventilation of the ocean interior in the EG setup.

Overall, an increasing isopycnal diffusivity makes the oceanic interior younger and high in CFC-11 concentrations, meaning an enhanced uptake of CFC-11. Thus the ocean ventilation becomes more and more with increasing isopycnal diffusivity (in setups K_{1000} , K_{2000}, and K_{5000}). In EG setup with parameterized isopycnal diffusivity, the interior of the ocean becomes older and has low CFC-11 concentrations, resulting in reduced tracer uptake and less ocean ventilation. In all the setups, the tracer uptake is higher in the Southern Ocean, meaning that the Southern Ocean is getting much more ventilated than the other oceanic basins.

5.4 Outlook

The analysis presented in this thesis on the sensitivity of the overturning circulation and the uptake of active and passive tracers to the changes in isopycnal diffusivity shows that the choice of isopycnal diffusivity in a model can potentially effect the results, and therefore our understanding of the changes in the circulation and tracer uptake. The CFCs used as passive tracers in the model in this thesis can be extended to include the CFCs beyond 1977 to understand the changes in tracer uptake over longer timescales. This is particularly important to understand the storage of anthropogenic tracers like Carbon, whose atmospheric concentrations steadily increase due to increasing emissions. Further, the model setup in this thesis can be further extended to understand the role of other factors in the tracer uptake in the ocean. One such factor is the wind stress, and a future step would be to extend the model setup to include the changes in wind stress to understand how the winds impact the tracer uptake and circulation. This also opens up the question of how isopycnal diffusivity and wind stress together impact the tracer uptake and circulation in the ocean.

Acknowledgments

I would like to express my deepest gratitude to Dr. Alexa Griesel for her kind supervision, guidance and encouragement throughout my research work. I would also like to thank Prof. Dr. Carsten Eden for his advice and lectures during the curriculum.

I would like to thank every single creature who helped me to come to this stage. It's been really beautiful, far more beautiful I'd ever thought it would be. I give special hearty thanks to my dearest and most adoring mother and my caring Manita, Lalli and my loving cat. I would like to extend my warm thanks to my friend whose music has helped me to grow.

Bibliography

Abernathey, R. and Ferreira, D. (2015). Southern ocean isopycnal mixing and ventilation changes driven by winds. *Geophysical Research Letters*, 42(23):10–357.

Canuto, V. and Dubovikov, M. (2006). Dynamical model of mesoscales in z-coordinates. *Ocean Modelling*, 11(1-2):123–166.

Danabasoglu, G. and Marshall, J. (2007). Effects of vertical variations of thickness diffusivity in an ocean general circulation model. *Ocean Modelling*, 18(2):122–141.

Danabasoglu, G. and Mc Williams, J. C. (1995). Sensitivity of the global ocean circulation to parameterizations of mesoscale tracer transports. *Journal of Climate*, 8(12):2967–2987.

Dutay, J.-C., Bullister, J. L., Doney, S. C., Orr, J. C., Najjar, R., Caldeira, K., Campin, J.-M., Drange, H., Follows, M., Gao, Y., et al. (2002). Evaluation of ocean model ventilation with cfc-11: Comparison of 13 global ocean models. *Ocean Modelling*, 4(2):89–120.

Eden, C. (2016). Closing the energy cycle in an ocean model. *Ocean Modelling*, 101:30–42.

Eden, C. and Greatbatch, R. J. (2008). Towards a mesoscale eddy closure. *Ocean Modelling*, 20(3):223–239.

Eden, C. and Olbers, D. (2014). An energy compartment model for propagation, nonlinear interaction, and dissipation of internal gravity waves. *Journal of Physical Oceanography*, 44(8):2093–2106.

Eden, C. and Olbers, D. (2017). A closure for internal wave-mean flow interaction. Part B: Wave drag. *Journal of Physical Oceanography*, (2017).

Fu*c*kar, N. S. and Vallis, G. K. (2007). Interhemispheric influence of surface buoyancy conditions on a circumpolar current. *Geophysical Research Letters*, 34(14).

Gent, P. R. and Mcwilliams, J. C. (1990). Isopycnal mixing in ocean circulation models. *Journal of Physical Oceanography*, 20(1):150–155.

Gent, P. R., Willebrand, J., McDougall, T. J., and McWilliams, J. C. (1995). Parameterizing eddy-induced tracer transports in ocean circulation models. *Journal of Physical Oceanography*, 25(4):463–474.

Gnanadesikan, A., Griffies, S. M., and Samuels, B. L. (2007). Effects in a climate model of slope tapering in neutral physics schemes. *Ocean Modelling*, 16(1-2):1–16.

Griffies, S., Gnanadesikan, A., Dixon, K. W., Dunne, J., Gerdes, R., Harrison, M. J., Rosati, A., Russell, J., Samuels, B. L., Spelman, M. J., et al. (2005). Formulation of an ocean model for global climate simulations. *Ocean Science*, 1(1):45–79.

Griffies, S. M. (1998). The gent–mcwilliams skew flux. *Journal of Physical Oceanography*, 28(5):831–841.

Killworth, P. D. (1997). On the parameterization of eddy transfer part i. theory. *Journal of Marine Research*, 55(6):1171–1197.

Killworth, P. D. (2001). Boundary conditions on quasi-stokes velocities in parameterizations. *Journal of physical oceanography*, 31(4):1132–1155.

Kuhlbrodt, T., Griesel, A., Montoya, M., Levermann, A., Hofmann, M., and Rahmstorf, S. (2007). On the driving processes of the atlantic meridional overturning circulation. *Reviews of Geophysics*, 45(2).

Marshall, J. and Speer, K. (2012). Closure of the meridional overturning circulation through southern ocean upwelling. *Nature Geoscience*, 5(3):171–180.

Munday, D., Johnson, H., and Marshall, D. (2014). Impacts and effects of mesoscale ocean eddies on ocean carbon storage and atmospheric pco2. *Global Biogeochemical Cycles*, 28(8):877–896.

Olbers, D. and Eden, C. (2013). A global model for the diapycnal diffusivity induced by internal gravity waves. *Journal of Physical Oceanography*, 43(8):1759–1779.

Olbers, D. and Eden, C. (2017). A closure for internal wave-mean flow interaction. part a: Energy conversion. *Journal of Physical Oceanography*, (2017).

Olbers, D. and Visbeck, M. (2005). A model of the zonally averaged stratification and overturning in the southern ocean. *Journal of Physical Oceanography*, 35(7):1190–1205.

Olbers, D., Willebrand, J., and Eden, C. (2012). *Ocean dynamics*. Springer Science & Business Media.

Rintoul, S. R., Hughes, C. W., and Olbers, D. (2001). The antarctic circumpolar current system. In *International Geophysics*, volume 77, pages 271–XXXVI. Elsevier.

Sabine, C. L., Feely, R. A., Gruber, N., Key, R. M., Lee, K., Bullister, J. L., Wanninkhof, R., Wong, C., Wallace, D. W., Tilbrook, B., et al. (2004). The oceanic sink for anthropogenic co2. *science*, 305(5682):367–371.

Sallée, J.-B., Matear, R. J., Rintoul, S. R., and Lenton, A. (2012). Localized subduction of anthropogenic carbon dioxide in the southern hemisphere oceans. *Nature Geoscience*, 5(8):579–584.

Sévellec, F., Huck, T., and de Verdière, A. C. (2010). From centennial to millennial oscillation of the thermohaline circulation. *Journal of marine research*, 68(5):723–742.

Stewart, A. L., Ferrari, R., and Thompson, A. F. (2014). On the importance of surface forcing in conceptual models of the deep ocean. *Journal of Physical Oceanography*, 44(3):891–899.

Toggweiler, J. and Samuels, B. (1998). On the ocean's large-scale circulation near the limit of no vertical mixing. *Journal of Physical Oceanography*, 28(9):1832–1852.

Visbeck, M., Marshall, J., Haine, T., and Spall, M. (1997). Specification of eddy transfer coefficients in coarse-resolution ocean circulation models. *Journal of Physical Oceanography*, 27(3):381–402.

Waugh, D. W., Primeau, F., DeVries, T., and Holzer, M. (2013). Recent changes in the ventilation of the southern oceans. *science*, 339(6119):568–570.

Versicherung an Eides statt

Hiermit versichere ich an Eides statt, dass ich die vorliegende Arbeit im Studiengang Physikalische Ozeanographie selbstständig verfasst und keine anderen als die angegebenen Hilfsmittel –insbesondere keine im Quellenverzeichnis nicht benannten Internet-Quellen – benutzt habe. Alle Stellen, die wörtlich oder sinngemäß aus Veröfentlichungen entnommen wurden, sind als solche kenntlich gemacht. Ich versichere weiterhin, dass ich die Arbeit vorher nicht in einem anderen Prüfungsverfahren eingereicht habe und die eingereichte schriftliche Fassung der auf dem elektronischen Speichermedium entspricht.

Hamburg, 20.05.2019 Ashwita Chouksey